Pathogenic Profiles and Molecular Signatures of Antinuclear Autoantibodies Rescued from NZM2410 Lupus Mice

Zhiyan Liang,[1] Chun Xie,[1] Cui Chen,[1] Desi Kreska,[1] Kelvin Hsu,[1] Liunan Li,[1] Xin J. Zhou,[3] and Chandra Mohan[1,2]

[1]*Simmons Arthritis Research Center,* [2]*Center for Immunology, and* [3]*Department of Pathology, University of Texas Southwestern Medical School, Dallas, TX 75390*

Abstract

Two outstanding questions concerning antinuclear antibodies (ANAs) in lupus involve their pathogenic potential and their molecular signatures. To address these questions, a panel of 56 antinuclear and 47 nonnuclear binding monoclonal antibodies was rescued from four seropositive NZM2410 lupus mice. The monoclonals varied in their reactivity to nucleosomes, ssDNA, dsDNA, and glomerular substrate. A large fraction of the antibodies demonstrated apparent polyreactivity (to DNA, histones, and glomerular antigens) due to bound, DNase-1 sensitive nuclear antigenic bridges. Although nephrophilic immunoglobulin (Ig) M and IgG antibodies were the most pathogenic, the dsDNA-binding antibodies were modestly so; in contrast, antinucleosome antibodies were clearly not pathogenic. Compared with the nonnuclear antigen-binding monoclonal antibodies rescued from the same mice, ANAs exhibited increased utilization of VH5/7183 genes and highly cationic heavy chain (HC) CDR3 regions. Most intriguingly, the CDR3 regions of the ANAs exhibited alternating arginine/lysine peaks at H96, H98, and H100, with neutral troughs at H95, H97, and H99. To summarize, glomerular-binding anti-dsDNA antibodies appear to be the most pathogenic variety of lupus autoantibodies. The presence of an alternating charge pattern in their HC CDR3 regions appears to be a prominent hallmark of ANAs.

Key words: CDR3 • nucleosomes • anti-DNA • New Zealand mice • nephritis

Introduction

It is well accepted that antinuclear antibodies (ANAs), anti-DNA Abs in particular, constitute major effectors of pathology in lupus (1–8). Several papers have already demonstrated that anti-dsDNA Abs can potentially induce disease when transferred in vivo (4–8). However, it is not clear if antinucleosome Abs (which bind strongly to nucleosomes and histone–DNA complexes, but not to histone-free DNA) are also pathogenic. Although a subset of lupus patients harbor predominantly antinucleosome Abs (directed particularly to H2A–H2B–DNA complexes) in the striking absence of anti-dsDNA ANAs, this peculiar phenotype is perhaps the best diagnostic hallmark of drug-induced lupus (9–10). Importantly, patients with drug-induced lupus, as well as those with "idiopathic" lupus who bear antinu-

cleosome (but not anti-dsDNA) Abs, are relatively free of renal disease (11). Burlingame et al. and Amoura et al. have reported that antinucleosome Abs appear early in disease, both in humans and in mice with lupus (12–14). In contrast, anti-dsDNA Abs appear later as the disease progresses, showing better temporal association with renal disease. Recent studies in congenic models of lupus also support the aforementioned notion that antinucleosome Abs are not associated with disease, whereas anti-dsDNA Abs are. Thus, although B6.*Sle1* mice have high titers of antinucleosome Abs associated with minimal glomerulonephritis, B6.*Sle1.Sle3* and B6.*Sle1.FAS*[lpr] mice exhibit high titers of anti-dsDNA Abs, accompanied by severe glomerulonephritis (15–18). On the other hand, isolated studies have demonstrated that some antinucleosome Abs may indeed be pathogenic, under certain experimental contexts (19).

Abbreviations used in this paper: ANA, antinuclear antibody; BUN, blood urea nitrogen; HC, heavy chain; LC, light chain; pI, isoelectric point; rt, room temperature; SLE, systemic lupus erythematosus.

In addition to anti-DNA and antinucleosome Abs, antibodies specific for laminin, fibronectin, actinin, as well as polyreactive glomerulotrophic (or nephrophilic) Abs, have all been shown to be potentially pathogenic (for review see reference 4). However, we still lack a clear understanding of how these different Abs compare with each other in terms of their pathogenic potential. One of the goals of this work is to rescue these different autospecificities from the same lupus-afflicted mice and to directly compare their relative pathogenic capacities.

The second goal of this work is to elucidate the molecular signatures of ANAs. The few comprehensive papers that have attempted to directly compare ANAs with non-ANAs have invariably used Abs drawn from the Kabat Ab database as controls (for reviews see references 20–26). The use of the Kabat database yields a large number of control Abs to compare against. Although the studied ANAs have predominantly been rescued from the BWF1 and MRL/*lpr* strains, the Kabat collection of Abs has been predominantly drawn from Balb/c and C57BL/6 (B6) mice, which differ from the lupus-prone strains in their *Ig* allotype. In addition, the Kabat database harbors many clonal replicates, numerous antihapten Abs that are homogenous in sequence, as well as several nuclear antigen-reactive Abs. These peculiarities of the Kabat collection of Abs could potentially lead to a biased representation of the "normal" or non-ANA repertoire. Thus, the "molecular signatures" of ANAs that have been reported previously using the Kabat database as a control must be interpreted with caution. In this work, we generate a sizeable panel of ANAs and non-ANAs from the same strain (and the same mice) to decipher any molecular footprints that may be truly peculiar to ANAs.

We rescued monoclonal autoantibodies from a murine lupus strain whose antibody repertoire has never been examined before: the NZM2410 strain, which is an NZB/NZW recombinant inbred that develops lupus nephritis by 5–6 mo of age (27). A panel of 56 ANAs and 47 non-ANAs were rescued from seropositive NZM2410 mice. By studying the functional properties and sequence profiles of these Abs, we aim to advance our understanding of two critical aspects of ANAs: the pathogenic potential of different antigenic fine specificities and their molecular signatures.

Materials and Methods

Mice. Male and female NZM2410 mice were obtained from the Jackson Laboratories or from R. Singh (University of Cincinnati, Cincinnati, OH), and aged till 5–8 mo of age, when they were serotested and killed for fusion. 2–4-mo-old male NZW mice (Jackson Laboratories) were used as recipients for the in vivo pathogenicity assays. All mice were housed in a specific pathogen-free colony, following institutional guidelines.

Hybridoma Fusion and mAb Purification. Spleens were removed aseptically from 5–8-mo-old seropositive NZM2410 mice. Single cell suspensions of the splenocytes were added to the SP2/0 fusion partner, at a 5–7:1 ratio, in 50% PEG. After washing, the cells were suspended in "fusion medium" (DMEM supplemented with 25% SP2/0 culture supernatant, 20% horse serum, and 1× HAT) and plated at 5×10^5 cells/well. All wells

with single colonies were tested for Abs 7–10 d after fusion. Cells from positive wells were subcloned once more. 1 wk after the seeding, wells with single colonies were picked for Ab (i.e., total IgG or IgM) screening by ELISA. Positive wells were expanded, and multiple freezes were made. IgG Abs from monoclonal hybridoma culture supernatants were purified by precipitation with 50% ammonium sulfate, followed by affinity chromatography using protein A–Sepharose columns (Pierce Chemical Co.). IgM antibodies were concentrated from the hybridoma culture supernatants by precipitation with 50% ammonium sulfate. Ab concentration was determined using a Coomassie PLUS protein assay kit (Pierce Chemical Co.), and an isotype-specific ELISA, as described in the next paragraph.

ELISA for Ig. The isotypes of the monoclonal antibodies were determined by ELISA and sequence confirmation. In brief, for the isotype-specific sandwich ELISA, goat anti–mouse IgM or goat anti–mouse IgG (Roche) was first coated onto plates (Immulon I; Dynatech) and blocked. Test samples were diluted serially and added to the plates for 2 h at rt (room temperature). Bound immunoglobulin was revealed with alkaline phosphatase–conjugated goat anti–mouse IgM, IgG1, IgG2a, IgG2b, or IgG3 antibodies (Roche or Jackson ImmunoResearch Laboratories) using p-nitrophenyl phosphate as a substrate. Concentrations were determined using a standard curve constructed using purified Ab standards (Sigma-Aldrich).

Assay for Specific Antibodies. mAbs were diluted up to 1 μg/ml and tested by both antinuclear immunofluorescence and ELISA as described previously (15–17). The antinucleosome ELISA was performed with a commercially available kit (KMI Diagnostics) using calf thymus nucleosome as substrate. The glomerular-binding ELISA was performed as described previously (16, 17) using sonicated rat glomeruli as substrate. In brief, renal cortices of Lewis rats were minced and pressed through a series of sieves of decreasing pore size (250, 150, and 75 μm). The glomeruli were collected on the finest sieve and were >95% pure. The glomeruli were washed with cold PBS three times, sonicated for 7 min, and centrifuged at 2,000 g for 5 min. The supernatant was used as a substrate (at 10 μg/ml) for the antiglomerular Ab ELISA. Other antigen-specific ELISAs were performed by coating Immulon II plates with 10 μg/ml ovalbumin, 10 μg/ml thyroglobulin, 10 μg/ml lysozyme, or 1 μg/ml laminin (all obtained from Sigma-Aldrich).

For all ELISA assays, the background OD was subtracted to obtain the final ODs. For the binding strengths shown in Table I, ODs in the respective antigen-specific ELISAs were mapped onto a semi-quantitative scale. On this scale, "+" and "++" indicate that the antigen-specific OD values registered by the respective mAbs (assayed in the linear range of 1–10 μg/ml) were 0.2–0.5, or >0.5-fold higher, respectively, compared with the corresponding OD values recorded for "total Ig" assayed in parallel. ELISAs were repeated twice with each mAb, to ensure reproducibility of the specificity patterns.

DNase-1 Treatment Experiments. ELISA plates were coated with the desired antigens, and blocked as usual. Antigen-coated wells were treated with 50 μl of DNase-I (100 μg/ml; Calbiochem) in PBS containing 5 mM MgCl$_2$ and 2 mM CaCl$_2$ at 37°C for 1 h. Sham-treated wells were treated with buffer (PBS) only. After washing, the test samples were added to the DNase-1 or sham-treated wells. Alternatively, the test samples (i.e., the Abs) were treated with DNase-I (final concentration = 100 μg/ml) in PBS, containing 5 mM MgCl$_2$ and 2 mM CaCl$_2$ at 37°C for 1 h. EDTA (final concentration = 5 mM) was added to terminate the DNase-I reaction. The total mixture was added to the ELISA

plates. The rest of the procedure was the same as for the standard ELISA as aforementioned. With both treatment approaches, any residual Ag reactivity was compared with that observed in the sham-treated controls.

In Vivo Pathogenicity Assays. We initially experimented with the injection of whole hybridoma cells; however, this approach yielded rather irreproducible results due to variability in the following parameters: (a) variable release of ANAs by the hybridoma cells in vivo; (b) variable release of apoptotic material by dying hybridoma cells in vivo; and (c) variable degree of tumorlike expansion of the hybridoma cells, leading to morbidity and mortality (unpublished data). Because one of the central goals of this work was to ascertain the relative pathogenicity of ANAs of different fine specificities, the pathogenicity studies were designed to minimize or exclude any other factors that may potentially impact disease outcome or confound data interpretation. In particular, attention was paid to the following three factors. First, because injection of whole hybridoma cells resulted in highly variable outcomes as aforementioned, only defined amounts of concentrated or purified mAb was used for the in vivo studies. Second, urinary protein was measured over 24 h using metabolic cages instead of performing single time point Dipstick tests because the former approach turns out to be far more quantitative and reliable. Third, all outcome measures (proteinuria, blood urea nitrogen [BUN], and histology) were performed in a blinded fashion.

2–4-mo-old male NZW mice were used as recipients for the mAb injection studies. The NZW strain shares 75% of its genome with the NZM2410 strain, including the *H2* locus (28). Of practical importance, the NZW strain is free of serum ANAs, and breeds easily, unlike the NZM2410 derivative. In brief, recipient mice were administered 10 daily i.p. injections of the respective mAbs, at a dose of 150 μg/d in a volume of 100 μl, adapting a well-established protocol (29). All injected mice were killed 24 h after the last injection on D10, and examined for disease as detailed in the next paragraph. Although this 10-d Ab injection protocol is sufficient to induce proteinuria and azotemia, it did not inflict any significant morphological change in the end organs.

Monitoring Renal Disease. All mice challenged with mAbs were monitored for several parameters of renal disease. 24-h urine samples were collected from all mice on D0, D4, D7, and D10 using metabolic cages, with free access to drinking water. Urinary protein concentration was determined using the Coomassie PLUS protein assay kit (Pierce Chemical Co.). Serum samples were collected on D0 and D10, and BUN was determined using a urea nitrogen kit (Sigma-Aldrich), following the manufacturer's instructions. All surviving animals were killed on D11, and the kidneys were processed for light microscopy. Renal histopathology was assessed as described previously (30, 31).

Ab Sequencing. Hybridoma cells were lysed in TRIzol (GIBCO BRL) by repetitive pipetting. 1 ml of TRIzol was used for 5–10 × 10⁶ cells. Chloroform was added, followed by vigorous agitation, and incubation at rt for 2–5 min. After centrifugation, the upper aqueous phase was procured and incubated with isopropanol at rt for 10 min to precipitate the RNA. The RNA pellet was centrifuged down, washed with 75% ethanol, air-dried, and dissolved in 0.1% diethylpyrocarbonate water (Sigma-Aldrich). RNA concentration and purity were gauged using $OD_{260/280}$ absorbance. RT-PCR was performed on total RNA using a commercially available kit (Promega), following the manufacturer's instructions. The respective heavy chain (HC) and light chain (LC) sequences were PCR amplified from the cDNA using the following sense and antisense primers (IDT-DNA): V_H, 5′-AGGT(G/C)(A/C)A(A/G)CTGCAG(G/C)AGTC(A/T)GG-

3′; Cμ, 5′-CAGGGGGCTCTCGCAGGAGACGAGG-3′; Cγ, 5′-GGACAGGGATCCAGAGTTCC-3′; V_κ, 5′-CCAGATG-TGTGATGACCCAGACTCCA-3′; C_κ: 5′-GTTGGTGCAG-CATCAGC-3′; $V_{\lambda1}$, 5′-TCTCCTGGCTCTCAGCTCAG-3′; $V_{\lambda2}$, 5′-GCCATTTCCCAGGCTGTTGTGACTCAGG-3′; $V_{\lambda x}$, 5′-GAGCTTAAGAAAGATGGAAGCCA-3′; $C_{\lambda1}$, 5′-CTTC-AGAGGAAGGTGGAAACAGGGTG-3′; and $C_{\lambda2}$, 5′-GGT-GAG(A/T)GTGGGAGTGGACTTGGGC-3′.

PCR was performed over 35 cycles using the following parameters: 45 s at 94°C, 60 s at 58°C, and 90 s at 72°C. PCR products were gel purified using the QIAEX II gel extraction kit (QIAGEN), and direct sequenced using either the 5′ or 3′ primers and the PRISM Ready Reaction Dye Terminator sequencing kit (Applied Biosystems) on a sequencing machine (model ABI377; Applied Biosystems). Ambiguous sequences were resequenced. The Taq error rate was estimated to be ∼1 in 4,000 nucleotides, based on multiple rounds of sequencing the Cμ gene. All sequences have been deposited into GenBank/EMBL/DDBJ (accession nos. AY436915–AY437055).

Sequence Analysis and Statistics. All Abs in the ANA and non-ANA databases were "blasted" against the publicly accessible "Ig-Blast" database of mouse Ig sequences at the National Center for Biotechnology Information (NCBI; http://www.ncbi.nlm.nih.gov/igblast) to determine the closest germline gene of origin, and to identify potential mutations. The CDR position and numbering scheme adopted matched that used by the National Center for Biotechnology Information IgBlast database. The frequencies of antibody V/J gene usage and the respective frequencies of individual amino acid residues at each CDR position were compared between the groups using chi-square tests. Where applicable, the Fisher's exact test was applied. The different CDR regions were also compared with respect to their mean isoelectric point (pI) as described previously (25, 32). Intergroup comparisons of phenotypes after in vivo Ab injections were also performed using the Student's *t* test (paired, where appropriate). All statistical comparisons were performed using SigmaStat (Jandel Scientific).

Online Supplemental Material. Table S1 shows the V-, D-, and J-gene origins of arginine and lysine residues in the HC CDR3 regions of the ANAs and non-ANAs rescued from the NZM2410 mice. Indicated also are the orientations of the D-genes used in the respective CDR3 regions. Table S2 shows the frequencies of nongermline encoded nucleotides and amino acid residues in the CDR and framework regions of HC and LC of the NZM2410-derived ANAs and non-ANAs. Also indicated are the frequencies of silent and replacement mutations in the respective Ab groups. Online supplemental material is available at http://www.jem.org/cgi/content/full/jem.20030132/DC1.

Results

Specificity Profiles of Rescued ANAs. A total of 56 antinuclear Abs (Table I), and 47 nonnuclear Ag-reactive Abs were rescued from four seropositive NZM2410 mice (named NZM-A to NZM-D). The rescued ANAs from all four mice were truly polyclonal, with only a modest degree of oligoclonal expansion. Within each mouse panel, the mAbs have been ordered according to their nuclear antigen specificity profile, as follows (Table I): (a) Abs that reacted predominantly with histones and/or nucleosomes; (b) Abs that reacted predominantly with ssDNA; (c) Abs that reacted with dsDNA, but not histones; and (d) Abs that re-

Table I. *Specificities of Antinuclear mAbs Rescued from NZM2410 Mice*

Mice	mAb[a]	Isotype	Histone	Histone/DNA[b]	dsDNA	ssDNA
NZM-A	ZA3A8	IgM	+[c]	++	−	−
	ZA4E6	IgM	+	+	−	−
	ZA7F8	IgM	++	++	−	−
	ZA1B11	IgM	−	+	−	+
	ZA6A8	IgM	−	−	−	+
	ZA5E11	IgM	−	++	+	++
	ZA8C4	IgM	−	+	+	+
	ZA7H10 (b)	IgG2a	−	++	++	++
	ZA1E4	IgM	+	+	+	−
	ZA1E5 (a)	IgM	++	++	+	+
	ZA2D8 (a)	IgM	+	++	+	−
	ZA6C10	IgM	+	(+)	+	++
	ZA3F7 (b)	IgG2a	+	++	++	++
NZM-B	ZB7D12	IgM	+	++	−	−
	ZB7E10	IgG2a	++	++	−	−
	ZB2C11 (c)	IgM	++	++	−	−
	ZB4A12 (e)	IgM	++	++	−	−
	ZB7B1 (e)	IgM	++	++	−	−
	ZB4H7	IgM	+	−	−	−
	ZB7F11 (d)	IgM	++	++	−	−
	ZB10B6	IgM	−	+	−	−
	ZB5G11	IgM	+	−	−	+
	ZB9A6	IgM	+	−	−	+
	ZB1A7	IgG3	−	+	−	++
	ZB2E5	IgM	−	−	−	+
	ZB2F12	IgM	−	−	−	+
	ZB5D2	IgM	−	−	−	+
	ZB5F3	IgM	−	−	−	+
	ZB9G6	IgM	−	−	−	+
	ZB2G14	IgG2a	−	++	++	−
	ZB5D3	IgG2a	−	++	++	−
	ZB2F10	IgM	−	++	++	+
	ZB2G10	IgM	−	(+)	+	++
	ZB3C7	IgM	−	++	++	++
	ZB8A7	IgM	++	++	+	−
	ZB2C1	IgG2b	++	+	+	−
	ZB10C9	IgM	+	+	+	+
	ZB4E2 (c)	IgM	+	++	+	+
	ZB5B4	IgM	++	++	+	+
	ZB2D7 (d)	IgM	++	++	+	+
	ZB1D9	IgM	++	(+)	+	++
	ZB4D8 (d)	IgG1	++	++	++	++
	ZB7D7	IgM	++	++	++	++
	ZB1B11	IgG2a	++	++	++	++

Table I. *Specificities of Antinuclear mAbs Rescued from NZM2410 Mice (continued)*

Mice	mAb[a]	Isotype	Histone	Histone/DNA[b]	dsDNA	ssDNA
NZM-C	ZCE1	IgM	−	++	−	−
	ZCH1	IgM	−	−	−	+
	ZCA3	IgG1	−	++	++	++
	ZCF4	IgM	++	++	++	+
	ZCB1	IgM	+	++	+	++
NZM-D	ZDD2	IgM	++	++	−	−
	ZDB4	IgG2b	−	++	−	−
	ZDC1	IgM	−	++	++	++
	ZDC3	IgM	+	++	−	+
	ZDA3 (f)	IgM	++	+	−	++
	ZDB2 (f)	IgM	++	+	−	++
	ZDD1	IgG2a	−	++	++	++

[a]All nuclear antigen-reactive monoclonal hybridomas rescued from the four NZM2410 mice are listed, ordered according to their antigen-binding profile. The first two letters of each mAb refer to the NZM2410 mouse of origin. For example, "ZA" refers to the mouse NZM-A. The clonal relationships observed among the rescued hybridomas are indicated in parentheses. All mAbs listed demonstrated antinuclear fluorescence on Hep-2 cells, with the exception of ZB9G6 and ZB4E2 (in italics).

[b]There was a near-perfect concordance between the results of the antinucleosome ELISA and the antihistone/DNA ELISA, with a few exceptions shown in parentheses.

[c]Antigen reactivity was tested by ELISA. All OD values in the respective antigen-specific ELISAs were mapped onto a semi-quantitative scale. On this scale, "+" and "++" indicate that the antigen-specific OD values registered by the respective mAbs (assayed in the linear range of 1–10 μg/ml) were 0.2–0.5, or >0.5-fold higher, respectively, compared with the corresponding OD values recorded for "total Ig" assayed in parallel.

acted with all of the aforementioned Ags, including DNA and histones.

This spread of nuclear antigen fine specificity is illustrated by mAbs rescued from the NZM-B mouse. As evident from Table I, the top quarter of all rescued Abs from this mouse represented antihistone Abs. It is not surprising that this category of Abs also reacted with histone–DNA complexes and nucleosomes because these composite Ags also bear histone epitopes. There was a nearly perfect correlation between histone/DNA reactivity and specificity for nucleosomes, with a few exceptions as noted in parentheses in Table I. The second quarter of this panel reacted predominantly with ssDNA; most of these Abs did not bind histone–DNA complexes or nucleosomes, presumably because the DNA in these complexes is double stranded in conformation. The third quarter of this panel reacted with dsDNA (and hence with histone–DNA complexes and nucleosomes), but not with DNA-free histones. Finally, the
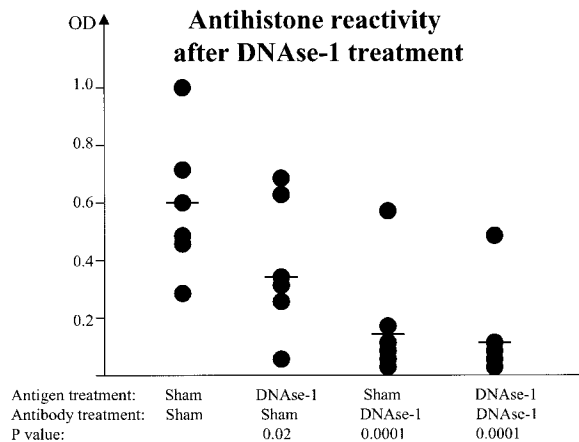
Antihistone reactivity after DNAse-1 treatment

Antigen treatment:	Sham	DNAse-1	Sham	DNAse-1
Antibody treatment:	Sham	Sham	DNAse-1	DNAse-1
P value:		0.02	0.0001	0.0001

Figure 1. Nuclear antigenic bridges facilitate histone binding by anti-DNA Abs. Six representative anti–dsDNA/antihistone dual-binding Abs were subjected to DNase-I or sham treatment as detailed in Materials and Methods. Likewise, the histone substrate (i.e., "Antigen") was also subjected to DNase-I or sham treatment. All Abs were tested for histone reactivity within the same ELISA plates. Horizontal bars represent the mean histone reactivity within each treatment group. The depicted p-values represent the result of comparing each group with the sham-treated (Ab and Ag) control. All DNase-I–treated Abs retained dsDNA-binding after treatment (not depicted).

last quarter of this panel showed reactivity to all of the tested antigens, including DNA and histones.

With respect to the latter specificity, potential dual reactivity to both histones and DNA seemed somewhat unlikely given the diametrically opposite polarities of these two antigens. One possibility was that the apparent reactivity to histones and/or DNA was mediated by nucleosomal Ags (originating, for example, from apoptotic hybridoma cells in culture) that were bound to the Ag-binding grooves of these mAbs; these moieties may have served as antigenic bridges facilitating contact with the DNA and/or histones coated on the ELISA plates. Thus, it was certainly conceivable that an anti-DNA or antinucleosome Ab might be masquerading as an antihistone Ab (or vice versa) through this mechanism. To ascertain if this phenomenon was indeed responsible for the observed dsDNA/histone dual reactivity, six representative dual-reactive ANAs were subjected to DNase-I treatment to digest away any bound nucleosomal material before reassaying their reactivity to dsDNA and/or histones. DNase-1 treatment of the Ab abrogated the ability of most of these "dual-reactive" Abs to bind histones (Fig. 1), but not to dsDNA (not depicted), suggesting that a substantial fraction of the apparent antihistone reactivity in the sera of these mice may be attributed to dsDNA-specific Abs. Interestingly, ~10–20% of the mAbs appeared to retain a certain degree of histone reactivity despite DNase-1 treatment of both the Ab and the antigenic substrate used for ELISA. It is currently unclear if these few clones represented true histone/DNA dual-reactive Abs, or whether the observed reactivity pattern was due to residual,

DNase-1–resistant, nucleosomal fragments tightly bound within the Ag-binding pockets of these Abs.

Nephrophilicity of Rescued Monoclonal Antibodies. In addition to being dsDNA reactive, sera from lupus mice are well recognized to be highly nephrophilic. To examine this at

A Percentage of NZM2410-derived ANAs that were nephrophilic

B **Antiglomerular reactivity after DNAse-1 treatment**

Antigen treatment:	Sham	Dnase-1	Sham	Dnase-1
Antibody treatment:	Sham	Sham	Dnase-1	Dnase-1
P value:		0.009	0.04	0.03
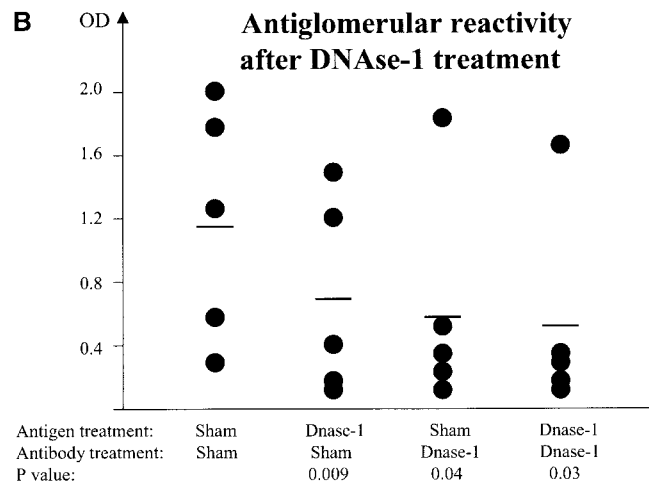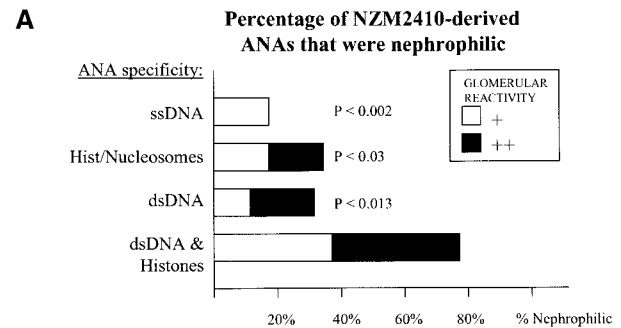
Figure 2. Glomerular reactivity of NZM2410-derived ANAs. (A) All the NZM2410-derived ANAs listed in Table I were tested for their reactivity to glomerular substrate as detailed in Materials and Methods. The 56 mAbs studied may be categorized into four groups according to their predominant Ag specificity pattern: anti-ssDNA Abs ($n = 11$), antihistone/nucleosome Abs ($n = 14$), nonhistone binding anti-dsDNA Abs ($n = 10$), and Abs that reacted with both histones and DNA ($n = 21$). In the composite bar graphs, the percentages of Abs within each group that tested positive for nephrophilicity are shown. (+ and ++) The glomerular antigen-specific reactivity (OD) of the respective mAbs (assayed in the linear range of 1–10 μg/ml) was 0.2–0.5, or >0.5-fold higher, respectively, compared with the corresponding OD values recorded for "total Ig," assayed in parallel. The percentage of dsDNA/histone dual binder Abs that also reacted with glomerular substrate was significantly higher than the corresponding percentages observed among anti-ssDNA ANAs ($P < 0.002$), antihistone/nucleosome Abs ($P < 0.03$), and the nonhistone-binding anti-dsDNA Abs ($P < 0.013$), as determined using the Fisher's exact test. (B) Five representative antiglomerular Abs (that also reacted with dsDNA) were subjected to DNase-I or sham treatment as detailed in Materials and Methods. Likewise, the glomerular substrate (i.e., Antigen) was also subjected to DNase-I or sham treatment. All Abs were tested for glomerular reactivity within the same ELISA plates. Horizontal bars represent the mean glomerular reactivity within each treatment group. The depicted p-values represent the result of comparing each group with the sham-treated (Ab and Ag) control.

the monoclonal level, the panel of antibodies listed in Table I was tested for glomerular reactivity by ELISA. A substantial fraction of these mAbs exhibited "nephrophilicity," with an interesting relationship to their nuclear antigen reactivity profile. As depicted in Fig. 2, ~80% of the histone/DNA dual binders listed in Table I had the capacity to bind glomerular substrate as well. In contrast, only ~20–30% of the mAbs in the other ANA specificity categories, and none of the non-ANAs exhibited glomerular reactivity. Glomerular binding observed in these in vitro assays could have

A 24-h urine protein (mg) in mice injected with IgG mAbs (○ D0, ● D10)

Monoclonal Ab:	ZB7A2	ZDB4	ZB1A7	ZB5D3	ZA7H10	ZB4D8	ZB1B11
Specificity							
Nucleosome	-	+	+	+	+	+	+
ssDNA	-	+	+	-	+	+	+
dsDNA	-	-	-	+	+	+	+
Glomeruli	-	-	-	-	-	+	+

been potentially mediated by one of two mechanisms. First, this could represent direct binding of the mAb to the glomerular substrate. Alternatively, this might not represent bona fide glomerular reactivity, but an apparent reactivity that is mediated by nucleosomal antigenic bridges, as aforementioned for histone binding. As observed for the histone reactivity experiments, it is interesting to note that a substantial fraction of the glomerular reactivity was abrogated by DNase-1 treatment of the Abs; only a minor fraction of the antiglomerular reactivity observed represented true DNA/glomerular dual reactivity (Fig. 2 B). Thus, together with the data in Table I and Fig. 1, a substantial fraction of the monoclonal ANAs rescued from NZM2410 mice demonstrated apparent "polyreactivity" to DNA, histones, and glomerular substrate as a consequence of Ab-bound nuclear material serving as antigenic bridges. However, these mAbs were not truly "polyreactive," because they lacked reactivity to several nonnuclear antigens tested, including ovalbumin, thyroglobulin, and lysozyme (unpublished data).

Pathogenic Potential of Rescued IgG Monoclonal Antibodies. Next, we gauged the in vivo pathogenicity of the IgM and IgG mAbs rescued from the NZM2410 mice. To ascertain if there was any relationship between the antigen reactivity profile of an Ab and its pathogenic potential, we first tested protein A purified IgG ANAs drawn from four different specificity groups as follows: (a) IgG non-ANAs that failed to bind any of the tested nuclear antigens or glomerular substrate; (b) IgG antinucleosome ANAs that bound histone–DNA complexes and nucleosomes, but not histone-free dsDNA; (c) IgG anti-dsDNA Abs that did not bind glomerular substrate; and (d) IgG ANAs that bound dsDNA as well as glomerular substrate.

As evident from Fig. 3 A, uninjected NZW mice typically excreted 0.4–1.0 mg urinary protein daily, with occasional mice excreting >1 mg/d. Clearly, the control non-ANA Ab as well as the IgG ANAs with reactivity to histone–DNA nucleosomal complexes and/or ssDNA (but not dsDNA) did not compromise renal function. In contrast, dsDNA-reactive IgG ANAs that lacked glomerular reactivity (i.e., ZB5D3 and ZA7H10) caused significantly increased proteinuria on D10, in the range of 1–1.5 mg/d. Interestingly, with both the histone/DNA–reactive Abs (ZDB4 and ZB1A7) and the dsDNA-reactive Abs (ZB5D3 and ZA7H10), concomitant reactivity to ssDNA did not affect the pathogenic potential of these Abs.

Most remarkably, IgG anti-dsDNA Abs with glomerular reactivity (i.e., ZB4D8 and ZB1B11) precipitated significant proteinuria (P < 0.0003) in the range of 1.5–2.5 mg/d on D10. In particular, the 24-h urinary protein levels in mice injected with IgG glomerular-binding anti-dsDNA ANAs (n = 10; mean = 1.88 mg/24-h) were significantly higher than the corresponding values in mice injected with IgG anti-dsDNA Abs (n = 10; mean = 1.30 mg/24-h; P < 0.003) on D10. Graphed in Fig. 3 B are the 24-h urine protein excretion levels recorded in the 10 mice injected with the IgG glomerular-binding anti-dsDNA ANAs (i.e., five mice injected with ZB4D8 and five mice injected with ZB1B11), as measured on D0, D3, D7, and D10.
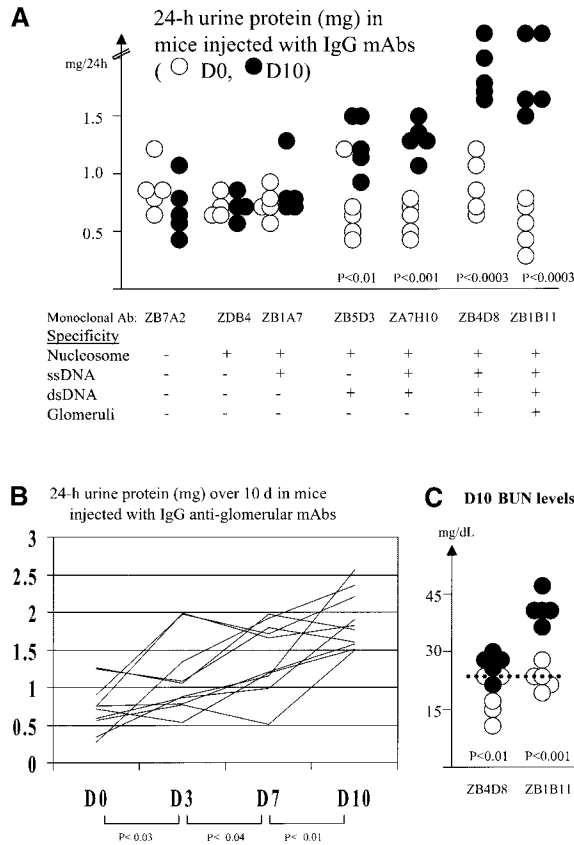
Figure 3. Renal pathogenicity of NZM2410-derived IgG ANAs. (A) Seven representative NZM2410-derived IgG mAbs were tested for in vivo pathogenicity as detailed in Materials and Methods. Although ZB4D8, ZDB4, and ZB1A7 were IgG1, IgG2b, and IgG3 in isotype, respectively, all other Abs were IgG2a in isotype. The specificity profiles of these Abs that have been tabulated below the figure were obtained from Table I. It should be noted that "+" in this figure simply indicates that the mAb reacts with the respective Ag, independent of the strength of reactivity. Both the beginning (D0, white dots), and ending (D10, black dots) 24-h urine protein levels (measured using metabolic cages) are depicted. Where the D10 proteinuria levels were found to be significantly higher than the corresponding D0 levels (using the Student's *t* test), the p-values are listed. (B) The 24-h urine protein excretion profiles of the 10 mice injected with IgG anti-dsDNA/glomerular dual binding Abs, ZB1B11 and ZB4D8, are depicted. 24-h urine protein measurements were performed on D0, D3, D7, and D10 after mAb administration. (C) The BUN levels measured on D0 and D10 after administration of the dsDNA/glomerular dual binding Abs, ZB4D8 and ZB1B11, are depicted. Depicted below each column of dots are the p-values calculated when the D0 and D10 BUN values were compared (using the Student's *t* test), and found to be significantly different. The dotted line refers to the mean D10 BUN level noted in all the other experimental groups of mice, combined.

A   24-h urine protein (mg) in mice injected with IgM mAbs

Monoclonal Ab:	ZB4G12	ZB7F11	ZB7D12	ZA7F8	ZDC3	ZA5E11	ZB7D7	ZDCl	ZCF4
Specificity									
Nucleosome	-	+	+	+	+	+	+	+	+
ssDNA	-	-	-	-	+	+	+	+	+
dsDNA	-	-	-	-	-	+	+	+	+
Glomeruli	-	-	-	+	+	-	+	+	+

B

Overall, these mice exhibited a progressive near-linear deterioration in renal function (as gauged by proteinuria) in a cumulative dose-dependent fashion. In addition, these mice had significantly higher BUN levels at the conclusion of the experiment, in contrast with the mice in the other treatment groups (Fig. 3 C).

Pathogenic Potential of Rescued IgM Monoclonal Antibodies. Next, a panel of nine IgM mAbs was selected for pathogenicity testing. As aforementioned, uninjected NZW mice excreted urinary protein of ≥1 mg/d. Clearly, IgM non-ANAs and Abs with reactivity restricted to histone–DNA nucleosomal complexes and/or ssDNA (but not dsDNA) did not compromise renal function significantly (Fig. 4 A). In contrast with the findings with the IgG ANAs, IgM Abs that were discordant in their reactivity patterns to dsDNA and glomeruli (e.g., ZA7F8, ZDC3, and ZA5E11) did not appear to be pathogenic. However, IgM Abs that had the potential to bind all of the aforementioned Ags, including dsDNA and glomerular substrate, were clearly pathogenic, leading to the excretion of 1–1.6 mg/d urinary protein (Fig. 4 A). Indeed, the D10 24-h urinary protein levels in the mice injected with these apparently polyreactive IgM Abs ($n = 13$; mean = 1.3 mg/24-h) were significantly higher than the D10 24-h urinary protein excretion levels observed in all other experimental groups combined ($n = 30$; mean = 0.9 mg/24-h; P < 0.0006). Finally, the mice in two of the three groups receiving dsDNA/glomeruli dual-reactive IgM Abs exhibited significantly elevated BUN levels at the conclusion of the experiments (Fig. 4 B).

Immunoglobulin Gene Usage by NZM2410-derived ANAs and non-ANAs. A second goal of this work was to elucidate the molecular signatures of ANAs. To achieve this, we compared the molecular profiles of the aforementioned NZM2410-derived ANAs with those of nonnuclear Ag-reactive Abs rescued from the same mice. HC and LC sequence information was successfully retrieved from 40 out of the 47 hybrids that exhibited no reactivity to ssDNA, dsDNA, histones, histone–DNA nucleosomal complexes, or to the glomerular substrate. These non-ANA Abs were also largely IgM in isotype, with most of the remainder being predominantly IgG2a in isotype (unpublished data). Thus, the overall isotype distribution was similar to that observed among the ANAs (Table I). For further molecular comparison of these non-ANAs with the aforementioned ANA panel, all clonal families were represented by one isolate each (to avoid any potential skewing of the data due to the expanded clones). All non-ANA mAbs sequenced were clonally independent, as indicated by their distinct HC CDR3 sequences. For each of the six clonal trees in the ANA panel (Table I, letters in parentheses), the most mutated member was retained for further comparative analysis. This reduced the sample size of ANAs to 49. Although the depicted data pertain only to datasets where the clonal siblings have been removed, inclusion of all clonal siblings did not impact the findings, owing perhaps to the modest degree of clonality seen among these mAbs (Table I).

As shown in Table II, Abs from both panels exhibited a fairly similar *VH* utilization profile, with *VH1/J558* predominating. Interestingly, there was significant overutilization of *VH5/7183* among the ANAs (P < 0.05), with this family being represented by at least six different germline genes (unpublished data). In particular, two out of these six *VH5* germline genes, *VH283* and *VH76–1BG*, together accounted for more than half of all the *VH5-*

Table II. *VH and Vk Family Usage by ANAs and Non-ANAs Derived from NZM2410 Mice*

	ANAs[a] (n = 49)	non-ANAs (n = 40)
	%	%
VH family		
VH1(J558)	55.1	75.0
VH2(Q52)	12.2	15.0
VH3(36-60)	2.0	0.0
VH4(X24)	0.0	0.0
VH5(7183)	26.5[b]	7.5
VH6(J606)	0.0	0.0
VH7(S107)	4.1	2.5
VH8(3609)	0.0	0.0
VH9(VGAM3.8)	0.0	0.0
VH10(VH10)	0.0	0.0
VH11(VH11)	0.0	0.0
VH12(VH12)	0.0	0.0
VH13(3609N)	0.0	0.0
VH14(SM7)	0.0	0.0
VH15(VH15)	0.0	0.0
Vk family		
Vk1	17.0	16.4
Vk2	8.5	3.7
Vk4/5	19.2	23.6
Vk8	4.3	5.5
Vk9/10	8.5	3.6
Vk12/13	6.4	3.6
Vk19/28	6.4	5.5
Vk20	0.0	1.8
Vk21	10.6	7.3
Vk23	10.6	14.6
Vk24/25	4.3	1.8
Vk32	0.0	1.8
Vk33/34	0.0	0.0
Vk38	0.0	5.5
VkRF	4.3	5.5

[a]All tabulated Abs are clonally independent. The antigenic fine specificities of the ANAs are listed in Table I. Of the 49 ANA hybridomas sequenced, 3 expressed V-λ LC; therefore, the depicted percentages pertain to LC sequence data obtained from 46 ANA hybrids.
[b]$P < 0.05$.

encoded ANAs rescued. With respect to the *Vk* utilization profile, the *Vk1* and *Vk4/5* families were the most frequently used in both the Ab panels, as noted for other ANAs and non-ANAs described previously (26). No further differences were noted when the nuclear antigen fine specificities of the ANAs were factored in. In addition, no

preferential copairing of any particular *VH* or *Vk* germline genes were noted that distinguished ANAs from non-ANAs (unpublished data).

Fig. 5 depicts the *Jk* utilization profiles of the NZM2410-derived ANAs and non-ANAs, as well as those of ANAs and non-ANAs described previously (26). Although the ANAs and non-ANAs derived from the NZM2410 mice did not differ significantly in terms of their *Jk* usage, both these groups of Abs had significantly higher *Jk5* utilization frequencies. Therefore, the *Jk5:Jk1* ratios in the NZM2410-derived ANAs (ratio = 1.2), and non-ANAs (ratio = 1.1), were significantly higher ($P < 0.013$ and $P < 0.006$, respectively) compared with the ANAs (ratio = 0.6) and non-ANAs (ratio = 0.4) drawn from the National Center for Biotechnology Information/ GenBank/EMBL/DDBJ databases. Factoring in the nuclear antigen fine specificities of the ANAs did not reveal any further differences. Thus, it is tempting to posit that these NZM2410-derived Abs (i.e., both the ANAs as well as the non-ANAs) may largely be the end product of a vigorous receptor-editing program at the *LC* locus. Nevertheless, one cannot exclude the possibility that other, yet to be defined, immunogenetic factors may be influencing *Jk* recombination in the NZM2410 genetic background.

CDR Lengths and Cationicity of NZM2410-derived ANAs. The CDR1, CDR2, and CDR3 sequences of NZM2410-derived ANA HC and LC are listed in Tables III and IV, respectively. The HC CDR3 lengths were not significantly different between these two groups of Abs (9.5 residues among the ANAs vs. 9.9 residues among the non-ANAs; $P > 0.05$). Likewise, no differences were noted in LC CDR1 lengths (13.5 residues vs. 12.6; $P > 0.05$). Previous papers comparing ANAs and non-ANAs have observed the CDR3 regions of ANA HC to be significantly more cationic (for reviews see references 20–25). In resonance with those observations, the mean pI value (averaged across the first six residues) of HC CDR3 was significantly higher among the NZM2410-derived ANAs compared with the non-ANAs (6.18 vs. 5.76; $P < 0.006$; Fig. 6). Interestingly, the CDR3 regions of ANAs demonstrated alternating peaks of significant cationicity at positions H96 ($P < 0.05$), H98 ($P < 0.01$), and H100 ($P < 0.05$), compared with the non-ANAs. The intervening positions at H95, H97, and H99 appeared to be uniformly neutral (with mean pI values hovering just below 6). In contrast, the non-ANAs were relatively neutral at most of these CDR3 positions and significantly more anionic at H98 (Fig. 6).

Residue Usage Differences in ANAs versus non-ANAs. Consistent with the pI profile differences portrayed in Fig. 6, NZM2410-derived ANAs exhibited significantly more "R" residues (9.4 vs. 3.8%, representing the mean percentages averaged across H95-H100a; $P < 0.02$) and significantly less "D" residues (5.8 vs. 10.5%; $P < 0.05$) in their HC CDR3 regions, compared with the non-ANAs. As is clear from Fig. 7 A, the NZM2410-derived ANAs exhibited peak usage of "R/K" residues (especially "R") at the alternating positions, H96, H98, and H100 (as well as
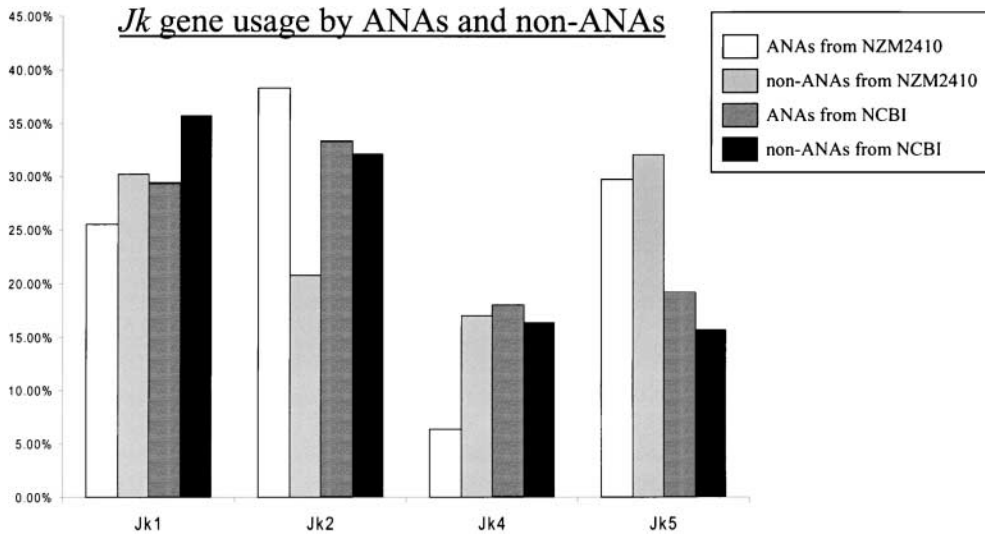
Figure 5. *Jk* usage frequencies among ANAs and non-ANAs. Indicated are the LC *Jk* usage frequencies of NZM2410-derived ANAs ($n = 46$), NZM2410-derived non-ANAs ($n = 40$), previously documented ANAs (from NCBI/GenBank/EMBL/DDBJ; $n = 264$), and non-ANAs (from NCBI/GenBank/EMBL/DDBJ; $n = 145$). The NCBI collection of ANAs and non-ANAs represents two new databases of LC sequences recently constructed and analyzed. The control ANAs represent 264 previously documented ANA LC sequences, drawn from 35 primary works, from which clonal replicates have been removed; they consisted of 139 anti-ss-DNA, 103 anti-dsDNA, and 22 antinucleosome Abs (26). The NCBI/GenBank/EMBL/DDBJ "non-ANAs" represent the LC sequences of 145 non-ANAs (with known antigen specificities) drawn from the NCBI/GenBank/EMBL/DDBJ database, with no overlapping target antigen specificities. Importantly, all clonal replicates have been removed from all four of the databases studied, so as to minimize any potential bias due to multi-member clones. The frequencies of *Jk5* among the NZM2410-derived ANAs and non-ANAs were significantly higher (P < 0.013 and P < 0.009, respectively) when compared with the corresponding frequencies observed among the NCBI-derived ANAs and non-ANAs.

H100a). In the intervening positions, H95, H97, and H99, the frequencies of R/K residues were outweighed by the corresponding frequencies of "D/E" residues. In contrast with the ANAs, the non-ANAs exhibited peak usage of anionic D/E residues (especially "D") at the same alternating positions, H96, H98, and H100. These reciprocal charge patterns at H96–H98 are highlighted using arrowheads in Fig. 7 A; these findings resonate well with the pI profile differences shown in Fig. 6.
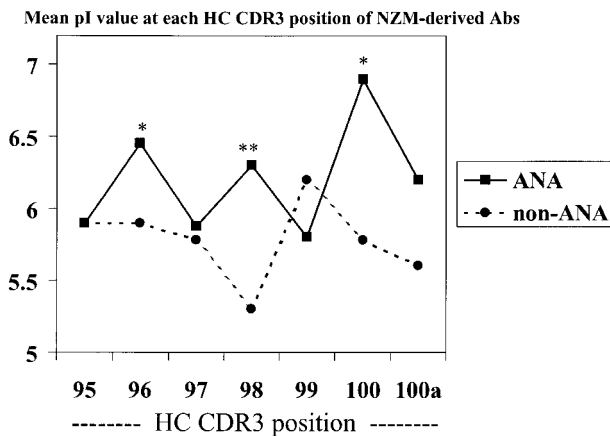
Figure 6. pI profiles across HC CDR3 regions of NZM2410-derived ANAs and non-ANAs. The mean pI value (isoelectric point) at each HC CDR3 position (from H95 to H100a) was calculated as detailed in Materials and Methods. As evident from Table III, few Abs had CDR3 residues beyond position H100a. The mean pI values observed among the NZM2410-derived ANAs ($n = 49$) and non-ANAs ($n = 40$) are plotted. Importantly, all clonal replicates have been removed from both databases. The pI values of the ANAs were systematically compared with the pI values of the non-ANAs at each indicated CDR position using the Student's *t* test (*, P < 0.05; **, P < 0.01).

Although the aforementioned charge motif was evident when all ANAs were examined in aggregate, no single ANA exhibited cationic residues at all three of the implicated CDR3 positions. However, several isolates demonstrated pairs of cationic residues at the alternating positions, H98 and H100, or H100 and H100b, including 3 out of 17 exclusive nucleosome binders, and 5 out of 28 dsDNA binders. Particularly impressive were the HC CDR3 regions of the dsDNA-reactive ANA, ZB2G14, which exhibited cationic residues at the alternating positions, H98, H100, and H100b. Although it would be important to ascertain if and how the anti-dsDNA/glomerular antibodies compared with the antinucleosome Abs, with respect to these signatures, no further differences were noted when the Abs were stratified by fine specificity (unpublished data).

Next, we analyzed the ANAs and the non-ANAs to gauge the molecular origins of the increased R/K residues in HC CDR3. Although the NZM2410-derived ANAs exhibited higher frequencies of D:D fusions (a feature that has been proposed by others as being an important contributor of CDR3 R residues), these differences were not statistically significant. As illustrated in Table S1 (available at http://www.jem.org/cgi/content/full/jem.20030132/DC1), the NZM2410-derived ANAs and non-ANAs did not differ in the genetic origins of their CDR3 R/K residues. Thus, in both groups of Abs, R/K residues at H95 were predominantly the result of V–D fusion (with N insertions), whereas R/K residues at H99–H100a were either D-gene encoded, or were the result of D–J recombination (with N insertions). Likewise, ANAs and non-ANAs did not differ in the D-gene reading frames they preferentially used, to encode the R/K residues (unpublished data). Thus, it is reasonable to posit that, although the molecular mechanisms that can potentially give rise to R/K residues

Table III. *Immunoglobulin Heavy Chain Usage by NZM2410-derived ANAs*

Mice	mAb[a]	Family	GL	Jh	CDR1[c] (31 32 33 34 35)	CDR2 (50 51 52 a 53 54 55 56 57 58 59 60 61 62 63 64 65)	CDR3 (95 96 97 98 99 100 a b c d e f i j k 101 102)
NZM-A	ZA3A8	S107	V11	1	D Y Y M S	L I R N N G Y T T E Y S A S A K G	E P Y G S S Y D – – – – – – – – –
	ZA4E6	7183	Vh283	2	N Y A M S	T I S S G G S Y T Y Y P D S V K G	P L T G Y – – – – – – – – Y F D Y
	ZA7F8	7183	Vh283	3	N Y A M S	T I D D G G S Y I S Y P D S V K G	P N Y G S S Y L – – – – – – F A Y
	ZA1B11	7183	7183.22b	4	D Y G M H	Y I S S G S S T I Y Y A D T V K G	D L L W L R R R – – – – Y A M D Y
	ZA6A8	36-60	36-60	2	S D Y M N	S I S Y – S G S T Y Y N P S L R S	S W A Y – – – – – – – – Y F D Y
	ZA5E11	J558	J558.c	1	S Y W M H	E I N P S N G G T N Y N E K F K S	G R – – – – – – – – – – – W Y F D V
	ZA8C4	J558	V130	2	D D Y M H	W I D P E N G D T E Y A S K F Q G	P Y G – – – – – – – – – – – – – –
	ZA7H10 (b)	J558	V23	2	S Y W M H	Y I N P S S G Y T E Y N Q K F K D	Y Y F G S S Y – – – – – – Y F D Y
	ZA1E4	J558	V102	1	G Y N W N	N I N P Y Y G S T S Y N Q K F K G	G N – – – – – – – – – – – W Y F D V
	ZA1E5 (a)	J558	V23	3	R Y W M H	E I N P S N G G T N F N E K F K S	G A N W D E W R – – – – – – F A Y
	ZA2D8 (a)	J558	V23	3	R Y W M H	E I N P S N G G S N S N E N F K N	G A N W D E W R – – – – – – F A Y
	ZA6C10	7183	Vh76-1BG	2	N Y A M S	T I S S G G S Y T Y Y P D S V K G	H G A G T – – – – – – – – Y F D Y
	ZA3F7 (b)	J558	V23	2	R Y W M H	Y I N P S S G Y T E Y N Q K F K D	Y Y Y G T I Y – – – – – – Y F D S
NZM-B	ZB7D12	7183	VH283	3	S Y G M S	T I S G G G G N T Y Y P Q S V K G	Y K A A R A T Y – – – – – W F A Y
	ZB7E10	Q52	Vox-1	3	S Y G V D	V I W G – G G N T N Y N S A F K S	D R G Y S H P – – – – – – – F A Y
	ZB2C11 (c)	J558	10B10.S	2	G Y N M H	Y I D P Y N G A T T Y N Q K F K G	G R P P A – – – – – – – – – – –
	ZB4A12 (e)	Q52	Vox1	3	S Y G V D	V I W G – G G N T N Y N S V F S S	D R G Y S Y P – – – – – – – F A Y
	ZB7B1 (e)	Q52	Vox1	3	S Y G V D	V I W G – G G N T N Y N S V L K S	D R G Y S Y P – – – – – – – F A Y
	ZB4H7	7183	7183.14	1	N Y D M S	T I S S G G S Y T Y Y P D S V K G	H G S S L – – – – – – – W Y F D V
	ZB7F11 (d)	J558	V23	2	T Y W M H	Y I N P S S G Y A D Y I Q K F K D	R E G R L R R G Y – – – – Y F D Y
	ZB10B6	J558	V6	1	S Y W M H	N I Y P G S S S T N Y N E K F K S	G A R A T H – – – – – W Y S D V
	ZB5G11	J558	J558.1	4	D Y Y M D	Y I Y P N N G G T S Y N Q K F K G	P G D W G – – – – – – – – A M D Y
	ZB9A6	J558	10B10.S	2	G Y N M N	N I N P Y Y G S T S Y N Q K F K G	P Y G Y D G G Y – – – – – Y F D Y
	ZB1A7	J558	MVARG2	2	N Y G I S	E I Y P R S G N T Y Y N E K F K G	E G R T V Y – – – – – – Y F D Y
	ZB2E5	J558	J558.c	3	S Y W M H	Y I N P S S A Y T E Y N Q K F K D	W G – – – – – – – – – – – – F A Y
	ZB2F12	J558	MVARG2	2	N Y G I S	E I Y P R S G N T F Y N E K F K G	R I G N – – – – – – – – – – Y
	ZB5D2	Q52	Vox-1	1	S Y A I S	V I W T – G G G T N Y N S A L K S	K G G N – – – – – – – Y W F D V
	ZB5F3	J558	VMU3.2	3	D Y Y M H	E I Y P G S G N T Y Y N E K F K G	D S Y Y G S C S – – – – – F A Y
	ZB9G6	J558	119.12	3	G Y Y M H	E I N P S T V S T T Y N Q N F K A	E G D W P – – – – – – – – F A Y
	ZB2G14	J558	V3	4	S Y W M H	K I D P S D S E T H Y N Q K F K D	S A L R L R T K P N E P – – M D Y
	ZB5D3	S107	V11	1	D Y Y M S	L I R N N G Y T T D Y R A S V K G	D S P L L R L R G – – – – Y F D Y
	ZB2F10	J558	V6	1	S Y W M H	K I D P S D S E T H Y N Q K F K D	R G P P Y – – – – – – – W Y F D V
	ZB2G10	J558	VMU3.2	3	S Y W M N	R I Y P G D G D T N Y N Q K F K G	G H S S G Y S – – – – – W F A Y
	ZB3C7	Q52	Vox-1	1	S Y G V H	V I W S – G G S T D Y N A A F I S	L G – – – – – – – – – – – Y F D V
	ZB8A7	7183	VH76-1BG	3	N Y A M S	T I S S G G T Y T F Y P D S V K G	H R D G Y S – – – – – – W F A Y
	ZB2C1	Q52	Vox1	1	S Y T I N	V I W T – G G G T N Y N S A L K S	I S P L L R L R N – – – W Y F D V
	ZB10C9	J558	VMU3.2	4	D Y Y I N	W I Y P G S G N T K Y N E K F K G	W V G S P – – – – – – Y A M D Y
	ZB4E2 (c)	J558	10B10.S	2	G Y N M H	Y I D P Y N G A T T Y N Q K F K G	G R P P A – – – – – – – – – – –
	ZB5B4	J558	V23	3	R Y W M H	E I N P S N Q Q T N F N E K F K S	G A N W D E W R – – – – – F A Y
	ZB2D7 (d)	J558	V23	2	S Y W M H	Y I N P S S G Y N D Y N Q K F K D	R E G R L R R G Y – – – – Y F D Y
	ZB1D9	Q52	Vox-1	3	S Y A I T	V I W T – G G G T N Y N S A L K S	G L Y Y G Y E A – – – – – W F A Y
	ZB4D8 (d)	J558	V23	2	T Y W M H	Y I N P S S G Y N D Y N Q K F K D	R E G R F R R G K – – – – Y F D Y
	ZB7D7	J558	119.12	4	G Y Y M H	E I N P R T G G T S Y N Q K F K A	G D L D – – – – – – – – – A M D Y
	ZB1B11	7183	7183.3b	3	N Y A M S	Y I S S G G Y S T Y Y P D S V K G	V V Y G E A – – – – – – – – A Y
NZM-C	ZCE1	J558	J558.1	2	D Y Y M N	R V N P S N G G T S Y N Q K F K G	A P L P Y – – – – – – – – Y F D Y
	ZCH1	J558	V102	3	T Y W I H	E I D P S D T Y T Y Y N Q K F K G	W G D G P – – – – – – – – F A Y
	ZCA3	7183	7183.3b	3	N Y A M S	F I S S G G D N T Y Y P D N V K G	P N Y V R S Y G – – – – – W F A Y
	ZCF4	J558	V130	3	D D Y I H	W I D P E N G D T E Y A S K F Q G	P Y G Y D L G R – – – – – F A Y
	ZCB1	7183	VH76-1BG	3	N Y A M G	T I S S G G I Y T Y Y P Q S V K G	L G L S S – – – – – – – – F A Y
NZM-D	ZDD2	J558	V130	3	D D Y L H	W I D P E N G D T E Y A S K F Q G	P L G R G – – – – – – – – F A Y
	ZDB4	J558	VMU3.2	2	S Y W M H	R I Y P R N G D A N Y N G E F K G	P L L R L R G – – – – – Y F D Y
	ZDC1	J558	V130	3	D Y Y M H	W I D P A N G D T E Y A S K F Q G	H Y Y G S T – – – – – – W F A Y
	ZDC3	J558	V23	1	S Y V M H	Y I N P Y N D G T K Y N E K F K G	D T T G S S S – – – – W Y F D V
	ZDA3 (f)	7183	7183.9	3	N Y A M S	T I S S G G S Y T Y Y P D S V K G	Q T Y G S S Y G – – – – – F A Y
	ZDB2 (f)	7183	7183.9	3	N Y A M S	T I S S G G S Y T Y Y P D S V K G	Q T Y G S S Y G – – – – – F A Y
	ZDD1	7183	VH283	3	N Y A M S	Y I S S G G G I T Y Y P D S L K G	G T G T G – – – – – – – – F A Y

[a]All mAbs are listed as ordered in Table I. Clonal membership is indicated using letters in parentheses.
[b]*VH* family and germline (GL) usage for each mAb are depicted.
[c]All CDR residues are shown. H52b and H52c have been omitted because only two Abs had residues at these positions.

Table IV. *Immunoglobulin Light Chain Usage by NZM2410-derived ANAs*

Mice	mAb[a]	V-κ usage[b]			CDR1[c]																	CDR2							CDR3								
		Family	GL	Jk	24	25	26	27	a	b	c	d	e	f	28	29	30	31	32	33	34	50	51	52	53	54	55	56	89	90	91	92	93	94	95	96	97
NZM-A	ZA3A8	Vk9/10	cp9	1	R	A	S	Q	G	I	S	N	–	–	–	–	–	–	Y	L	N	Y	T	S	S	L	H	S	Q	Q	Y	S	K	L	P	P	T
	ZA4E6	Vk23	23-39	5	R	A	S	Q	S	I	S	D	–	–	–	–	–	–	Y	L	H	Y	A	S	Q	S	I	S	Q	N	G	H	S	F	P	P	T
	ZA7F8	Vk23	23-48	4	R	A	S	Q	S	I	G	T	–	–	–	–	–	–	S	I	H	Y	V	S	E	S	I	S	Q	Q	S	N	S	W	H	S	R
	ZA1B11	Vk12/13	12-46	2	R	A	S	E	N	I	Y	S	–	–	–	–	–	–	N	L	A	A	A	T	N	L	A	D	Q	H	F	W	G	T	M		
	ZA6A8	Vk21	21-5	2	R	A	S	E	S	G	D	S	Y	–	–	S	D	S	Y	M	H	R	A	S	I	L	E	S	Q	Q	N	N	R	D	P	Y	T
	ZA5E11	Vk23	23-39	5	R	A	S	Q	S	I	S	D	–	–	–	–	–	–	Y	L	H	Y	A	S	Q	S	I	S	Q	N	G	H	S	F	P	L	T
	ZA7H10 (b)	Vk1	bb1	1	R	S	S	Q	S	L	V	H	S	–	N	G	N	T	Y	L	H	K	V	S	N	R	F	S	S	Q	S	T	H	V	P	R	T
	ZA1E4	Vk23	23-39	5	R	A	S	Q	S	I	S	D	–	–	–	–	–	–	Y	L	H	Y	A	S	Q	S	I	S	Q	N	G	H	S	F	P	L	T
	ZA1E5 (a)	Vk8	8-21	2	K	S	S	Q	S	L	L	N	S	R	T	R	K	N	Y	L	A	W	A	S	T	R	E	S	K	Q	S	Y	N	L	Y	–	T
	ZA2D8 (a)	Vk8	8-21	2	K	S	S	Q	S	L	L	N	R	R	T	R	K	N	Y	L	A	W	A	S	T	R	E	S	K	Q	S	Y	N	L	Y	–	T
	ZA6C10	VK4/5	ai4	1	T	A	S	S	S	V	S	S	S	–	–	–	–	–	Y	L	H	S	T	S	N	L	A	S	H	Q	Y	H	R	S	P	P	T
	ZA3F7 (b)	Vk1	bb1	1	R	S	S	Q	S	L	V	H	S	–	N	G	N	T	Y	L	H	K	V	S	N	R	F	S	S	Q	S	T	H	V	P	R	T
NZM-B	ZB7D12	Vk1	cr1	1	R	S	S	Q	S	I	V	H	S	–	N	G	N	T	Y	L	E	K	V	S	N	R	F	S	F	Q	G	S	H	V	P	P	T
	ZB7E10	Vk2	bd2	5	K	S	G	Q	S	L	L	D	S	–	D	G	K	T	Y	L	N	L	V	S	K	L	D	S	W	Q	G	T	H	F	P	L	T
	ZB2C11 (c)	Vk8	8-21	1	K	S	S	Q	S	L	L	N	S	R	T	R	K	N	Y	L	A	W	A	S	T	R	E	S	K	Q	S	Y	N	L	W	–	T
	ZB4A12 (e)	Vk2	bd2	5	K	S	G	Q	S	L	L	D	S	–	D	G	K	T	Y	L	N	L	V	S	K	L	D	S	W	Q	G	T	H	F	P	L	T
	ZB7B1 (e)	Vk2	bd2	5	K	S	S	Q	S	L	L	D	S	–	D	G	K	T	Y	L	N	L	V	S	K	L	D	S	W	Q	G	T	H	F	P	L	T
	ZB4H7	Vk9/10	ba9	5	K	A	S	Q	D	I	N	G	–	–	–	–	–	–	Y	L	S	R	A	N	R	L	V	D	L	Q	Y	D	E	F	P	L	T
	ZB7F11 (d)	VkRF	RF	5	R	A	S	K	S	I	S	R	–	–	–	–	–	–	Y	L	A	S	G	S	T	L	Q	S	L	Q	H	N	E	Y	P	L	T
	ZB10B6	Vk21	21-2	2	R	A	S	E	S	V	D	N	Y	–	–	G	I	S	F	M	N	A	A	S	N	Q	G	S	Q	Q	S	K	E	V	P	Y	T
	ZB5G11	Vk21	21-4	1	K	A	S	Q	S	V	D	Y	D	–	–	G	D	S	Y	M	N	A	A	S	N	L	E	S	Q	Q	S	N	E	D	P	P	T
	ZB9A6	Vk23	23-39	5	R	A	S	Q	S	I	S	D	–	–	–	–	–	–	Y	L	H	Y	A	S	Q	S	I	S	Q	N	G	H	S	F	P	L	T
	ZB1A7	Vk1	bb1	1	R	S	S	Q	S	L	V	H	S	–	N	G	N	T	Y	L	H	K	V	S	N	R	F	S	S	Q	S	T	H	V	P	R	T
	ZB2E5	Vk9/10	bv9	2	R	A	S	Q	D	I	G	S	–	–	–	–	–	–	S	L	N	A	T	S	S	L	D	S	L	Q	Y	A	S	S	P	Y	T
	ZB2F12	Vk1	cv1	2	K	S	A	K	S	L	L	N	S	–	D	G	F	T	Y	L	D	L	V	S	N	R	F	S	F	Q	S	N	Y	L	P	C	T
	ZB5D2	VK4/5	aq4	5	S	A	S	S	S	V	S	–	–	–	–	–	–	–	Y	M	C	L	T	S	N	L	A	S	Q	Q	W	S	S	N	P	L	T
	ZB5F3	Vk24/25	hf24	2	R	S	S	K	S	L	L	H	S	–	N	G	N	T	Y	L	Y	R	M	S	N	L	A	S	M	Q	H	L	E	Y	P	Y	T
	ZB9G6	Vk19/28	19-14	2	K	A	S	Q	N	V	R	T	–	–	–	–	–	–	A	V	A	L	A	S	I	R	H	T	L	Q	H	W	N	Y	P	Y	T
	ZB2G14	Vk2	bd2	2	K	S	S	Q	S	L	L	D	S	–	D	G	K	T	Y	L	N	L	V	S	K	L	D	S	W	Q	G	T	H	F	P	H	T
	ZB5D3	Vk1	bb1	2	R	S	S	Q	S	L	V	H	S	–	N	G	N	T	Y	L	H	K	V	S	N	R	F	S	S	Q	S	T	H	V	P	Y	T
	ZB2F10	Vk24/25	hf24	2	R	S	S	K	S	L	L	H	S	–	N	G	N	T	Y	L	Y	R	M	S	N	L	A	S	M	Q	H	L	E	Y	P	Y	T
	ZB2G10	Vk12/13	12-44	1	R	A	S	E	N	I	Y	S	–	–	–	–	–	–	Y	L	A	N	A	K	T	L	A	E	Q	H	H	Y	G	T	P	W	T
	ZB8A7	Vk9/10	cp9	2	S	A	S	Q	G	I	S	N	–	–	–	–	–	–	Y	L	N	Y	T	S	N	L	H	S	Q	Q	Y	S	K	L	P	Y	T
	ZB10C9	Vk4/5	ai4	2	T	A	R	S	S	V	S	S	S	–	–	–	–	–	Y	L	H	S	T	S	N	L	A	S	H	Q	Y	H	L	S	P	Y	T
	ZB4E2 (c)	Vk8	8-21	1	K	S	S	Q	S	L	L	N	R	R	F	T	Q	N	Y	L	G	W	A	S	T	R	E	S	K	Q	S	Y	N	L	W	–	T
	ZB5B4	Vk8	8-21	2	K	S	S	Q	S	L	L	N	S	R	T	R	K	N	Y	L	A	W	A	S	T	R	E	S	K	Q	S	Y	N	L	Y	–	T
	ZB2D7 (d)	VkRF	RF	5	R	T	S	K	S	I	S	K	–	–	–	–	–	–	Y	L	A	S	G	S	T	L	Q	S	Q	Q	H	N	E	Y	P	L	T
	ZB1D9	Vk4/5	kf4	5	C	A	S	S	S	I	S	S	N	–	–	–	–	–	Y	L	H	R	T	S	N	L	A	S	Q	Q	G	S	S	I	P	L	T
	ZB4D8 (d)	Vk9/10	ba9	4	K	A	S	Q	S	D	K	D	–	–	–	–	–	–	Y	L	S	Y	A	A	N	L	A	D	Y	N	M	V	R	A	V	–	T
	ZB7D7	Vk4/5	ai4	2	T	A	R	S	S	V	S	S	S	–	–	–	–	–	Y	L	H	S	T	S	N	L	A	S	H	Q	Y	H	L	S	P	Y	T
	ZB1B11	Vk1	bb1	2	R	S	S	Q	S	L	V	H	S	–	N	G	N	T	Y	L	H	K	V	S	N	R	F	S	S	Q	S	T	H	V	P	Y	T
NZM-C	ZCE1	Vk19/28	19-14	5	K	A	S	Q	N	V	R	T	–	–	–	–	–	–	A	V	A	Y	A	S	N	R	H	T	L	Q	H	W	N	Y	P	L	T
	ZCH1	Vk4/5	aa4	1	S	A	S	S	S	V	S	–	–	–	–	–	–	–	Y	M	Y	R	T	S	N	L	A	S	Q	Q	Y	H	S	Y	P	P	T
	ZCA3	VkRF	RF	5	R	A	S	K	S	I	S	R	–	–	–	–	–	–	Y	L	A	S	G	S	T	L	Q	S	Q	Q	H	N	E	C	P	L	T
	ZCF4	Vk4/5	ai4	2	T	A	S	S	S	V	S	S	S	–	–	–	–	–	Y	L	H	S	T	S	N	L	A	S	H	Q	Y	H	R	S	P	P	T
	ZCB1	Vk1	bb1	2	R	S	S	Q	S	L	V	H	S	–	N	G	N	T	Y	L	H	K	V	S	N	R	F	S	S	Q	S	T	H	V	P	Y	T
NZM-D	ZDD2	Vk21	21-10	1	R	A	S	E	S	V	D	S	F	–	–	D	N	S	F	M	Y	L	T	S	N	L	E	S	Q	Q	N	N	E	D	P	W	T
	ZDB4	Vk21	21-5	1	R	A	S	E	S	V	D	S	Y	–	–	G	N	S	F	M	H	R	A	S	N	L	E	S	Q	Q	S	N	E	D	P	R	T
	ZDC1	Vk1	bb1	4	R	S	S	Q	S	L	V	H	S	–	N	G	N	T	Y	L	H	K	V	S	N	R	F	S	S	Q	S	T	H	V	P	F	T
	ZDC3	Vk2	bd2	5	K	S	S	Q	S	L	L	D	S	–	D	G	K	T	Y	L	N	L	V	S	K	L	D	S	W	Q	G	T	H	F	P	–	T
	ZDA3 (f)	Vk4/5	ay4	5	R	A	S	S	S	I	S	S	N	–	–	–	–	–	Y	L	H	R	T	S	I	L	A	S	Q	Q	G	S	S	S	P	P	R
	ZDB2 (f)	Vk4/5	ai4	2	T	A	S	S	S	V	S	S	S	–	–	–	–	–	Y	L	H	T	T	S	N	L	A	S	H	Q	Y	H	R	S	P	Y	T
	ZDD1	Vk19/28	19-23	1	K	A	S	Q	D	V	G	T		–	–	–	–	–	A	V	A	W	A	S	T	R	H	T	Q	Q	Y	S	S	Y	P	R	T

[a] All mAbs are listed as ordered in Table I. Clonal membership is indicated using letters in parentheses. The entries for ZB3C7, ZB2C1, and ZA8C4 have been omitted because these mAbs used λ LCs.

[b] The *Vk* family and germline (GL) gene usage for each mAb are depicted.

[c] All CDR residues, following the numbering scheme adopted by the National Center for Biotechnology Information/IgBlast, are shown.
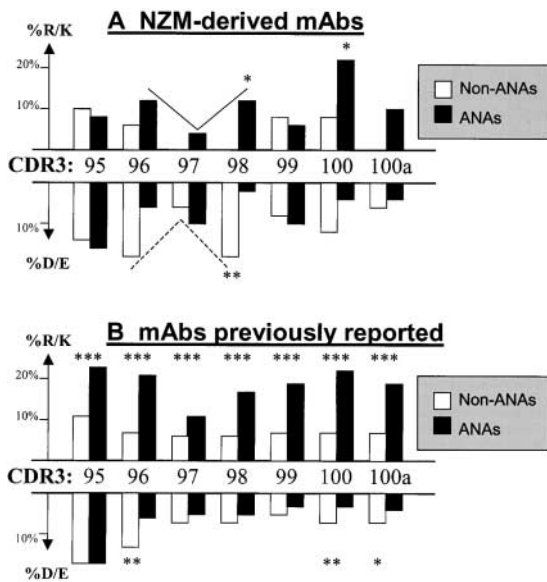
Figure 7. The distribution of "R/K" and "D/E" residues in the HC CDR3 regions of ANAs and non-ANAs. In A, the respective frequencies of R/K and D/E residues at each of the HC CDR3 positions, H95–H100a, among the NZM2410-derived ANAs ($n = 49$) and non-ANAs ($n = 40$) are depicted. Differences (between ANAs and non-ANAs) that attained statistical significance are denoted (*, $P < 0.05$; **, $P < 0.01$). The solid line arrowhead indicates the alternating frequency peaks of cationicity between H96 and H98 of ANAs; the dotted line arrowhead indicates the alternating peaks of anionicity between H96 and H98 among the non-ANAs. There were too few sequences with CDR3 positions extending beyond H100a (Table III). In B, a similar analysis was performed using previously reported ANAs ($n = 269$) and non-ANAs ($n = 3,600$) (for review see reference 25). These control ANAs represent 269 previously documented ANAs drawn from 35 primary works, from which clonal replicates have been removed; they consisted of 143 anti-ssDNA, 103 anti-dsDNA, and 23 antinucleosome Abs (25). The control "non-ANAs" represent the HCs of all Abs deposited in the Kabat database. Differences that attained statistical significance are denoted (*, $P < 0.05$; **, $P < 0.01$; ***, $P < 0.001$).

in the HC CDR3 regions of ANAs and non-ANAs are fairly similar, the increased frequency of such residues observed among the ANAs is likely to be the consequence of antigen-driven selection.

Comparative analyses of previously rescued ANAs have also revealed (less prominently) differences in the other CDR regions (for review see reference 25). However, the CDR1 and CDR2 regions of the NZM2410-derived ANAs and non-ANAs were very similar, with only one difference attaining statistical significance. Thus, the ANAs exhibited an increased frequency of "S" residues at the CDR2 position, H52, compared with the non-ANAs ($P < 0.05$). In reviewing the origin of this specific difference, it was clear that this difference was entirely due to the increased usage of *VH5/7183 VH* genes (that exhibited germline-encoded S residues at H52), among the ANAs, as depicted in Table II. Although there was a trend toward increased N residues at H31 and reduced D residues at H52–H56 among the ANAs (as noted previously in other ANAs; reference 25), these differences fell short of statistical significance. Finally, no significant residue usage differ-

ences were noted in the LC of ANAs, compared with those of non-ANAs.

Contributions of Somatic Mutation. Somatic mutation has been accorded an important role in the generation of ANAs (33, 34). As summarized in Table S2 (available at http://www.jem.org/cgi/content/full/jem.20030132/DC1), very little somatic mutation was noted in the LC and the framework regions of the HCs, in both groups of Abs; in contrast, the HC CDR1 and CDR2 regions of both the ANAs and the non-ANAs exhibited high mutation frequencies, with high replacement/silent ratios. In addition, the mutation frequencies did not differ significantly between the two groups of Abs, when individual positions within the CDR1 and CDR2 regions were examined (Table S2). However, three HC CDR positions were of particular interest. H31, H50, and H56 of ANAs exhibited the highest mutation frequencies ($>40\%$). More interestingly, the replacement mutations at these three positions resulted in a spectrum of amino acids that were quite different from those seen at the corresponding positions of non-ANAs. Although 70% of the mutations at H31 were to N or R residues among the ANAs, the corresponding value was 36% among the non-ANAs ($P > 0.05$). Likewise, ANAs exhibited more mutations to Y residues at H50 ($P < 0.01$), and more mutations to "N/Y" residues H56 ($P > 0.05$), compared with the non-ANAs. Although these trends were interesting, most fell short of statistical significance. Clearly, larger datasets must be analyzed to investigate these differences further. When we next examined the codons that had been used to encode the aforementioned amino acid residues, interesting, but similar, patterns were observed in both groups of Abs. For example, in both the ANAs and the non-ANAs, R and N residues at H31 were invariably the product of a single nucleotide mutation of "AGC" (that encodes for "S"), which is germline-encoded at the H31 position of several germline genes belonging to the *VH1/J558* (e.g., *V23, MVARG2*, etc.) and *VH5/7183* (e.g., *VH76–1BG, VH283, 7183.3b*, and *7183.9*, etc.) *VH* families.

Finally, we examined the multimember clonal families among the rescued ANAs. Of the six clonal families observed, five consisted of two to three nonidentical members each (Fig. 8), whereas the remaining clone (Table I, clone "f") consisted of two identical isolates. This was consistent with the mutation frequencies listed in Table VI, whereas the HC of these clones displayed high mutation frequencies, particularly in the CDR regions, the LC varied little from the germline sequences, for the most part. In contrast to clones "A," "B," and "E," clones "C" and "D" exhibited intraclonal differences in ANA fine specificity. Because both members of clone C possessed the same germline-encoded *VH1/J558 10B10S* germline gene, the few LC mutations exhibited by clone 4E2 must have been responsible for the dsDNA reactivity profile of this clone. In this context, the replacement mutation at L27e, which results in an R residue, is particularly attractive. This is perhaps the first example of an instance where somatic mutation of the LC partner may have been re-

Clone A   Clone B   Clone C   Clone D   Clone E

[Figure 8 diagram showing heavy chain and light chain somatic mutations for clones A–E]
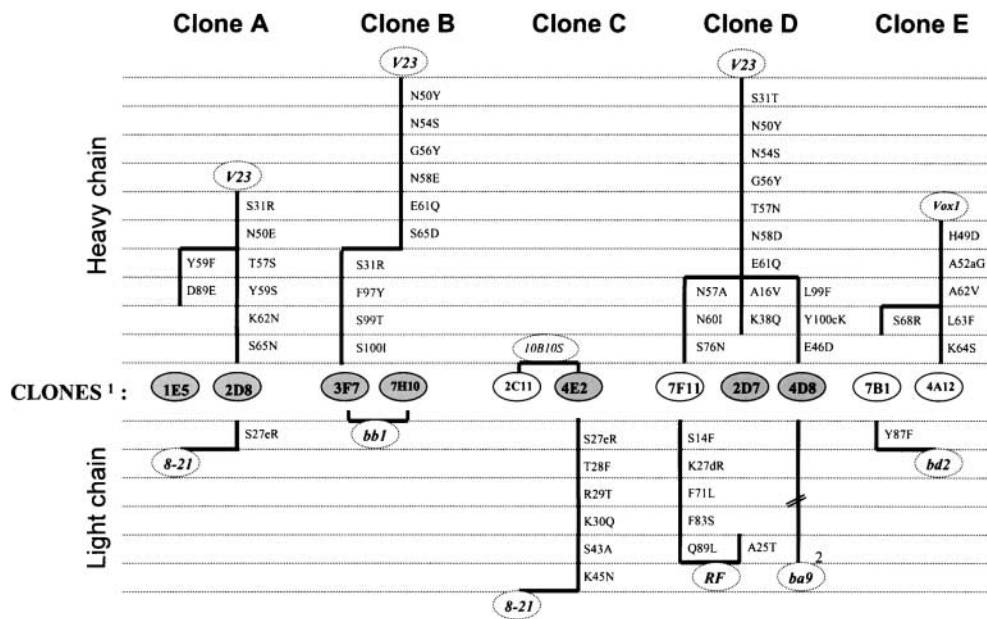
Figure 8. Somatic variations between members of antibody clones. 11 NZM2410-derived monoclonal ANAs are depicted that belonged to five independent clones, A–E, as indicated in Tables I, III, and IV. These clones have been labeled the same way as in Table I, except that the mouse origin identifiers (e.g., "ZA", "ZB," etc.) have been omitted. DsDNA-reactive clones are shaded in gray, whereas exclusive nucleosome binders are left unshaded. (top) The HC somatic mutations relative to the closest HC germline gene (indicated in oval labels with dotted borders) are depicted. (bottom) The LC somatic mutations relative to the closest LC germline gene (indicated in oval-shaped labels with dotted borders) are depicted. Thus, in clone "B," mAbs 7H10 and 3F7 vary from the *J558* germline gene, *V23*, by 6 or 10 residues, respectively, whereas they both bear the same unmutated LC *Vk1* germline gene, *bb1*. Interestingly, whereas the first-listed two members of Clone D, 7F11 and 2D7, possessed a mutated *RF Vk* germline gene, the third member possessed an entirely different LC gene that differed from the *Vk9* germline gene, *ba9*, by nine somatic mutations (not depicted).

sponsible for generating a dsDNA binder, beginning with a nucleosome-restricted precursor.

Clone D is also very intriguing, in view of its LC diversity. The strong dsDNA-binder, 4D8, is the most mutated member of this clone, as it bears a *V23* germline gene with 10 HC mutations, and a *Vk9* germline gene (recombined to *Jk4*), with 9 somatic mutations. Because its clonal siblings, 7F11 and 2D7, were recombined to *Jk5* and possessed fewer LC mutations, and because they did not bind dsDNA (7F11), or bound dsDNA weakly (2D7), it is tempting to speculate that 7F11 and 2D7 may be the products of LC receptor editing, beginning with the dsDNA-binding 4D8 clone as a precursor. Therefore, one might posit that LC receptor editing may potentially play a role in generating antinucleosome specificities, beginning with a dsDNA binder. Clearly, these suggestions are speculative, and need to be tested using in vitro expression and mutagenesis studies.

Discussion

Although it is well established that anti–dsDNA Abs play a cardinal role in the development of lupus, the pathogenic potential of two closely associated specificities, antinucleosome Abs and antiglomerular Abs, have remained unclear. As discussed earlier, antinucleosome ANAs have been documented in several murine models and clinical contexts where end organ disease was distinctly absent (9–13). Although these analyses support the notion that antinucleosome Abs that do not bind dsDNA may not be pathogenic, isolated papers in experimental models have suggested that these Abs may have the potential to induce renal disease when complexed with nuclear antigens (19). In contrast to

anti–dsDNA and antinucleosome ANAs, an overlapping specificity that is fairly well documented to be associated with renal disease is the group of Abs that exhibit nephrophilicity (4, 35, 36). Although the existence of these three sets of specificities (anti–dsDNA, antinucleosome, and antiglomerular Abs) have been well recognized for some time, little effort has been expended to directly compare the relative pathogenic capacities of these different specificities. In particular, we sought to address two pressing questions in this work as follows: (a) Are anti–dsDNA Abs more pathogenic than antinucleosome Abs? and (b) Are glomerular-binding ANAs more pathogenic than their nonnephrophilic counterparts?

To address these questions, we took advantage of the observation that NZM2410 lupus mice exhibited all three serological specificities. As summarized in Figs. 3 and 4, the answers to both those questions were in the affirmative. First, antinucleosome Abs of both IgM and IgG isotypes were relatively innocuous, in comparison to anti–dsDNA ANAs. Second, although dsDNA–reactive Abs appeared to be fairly pathogenic, the presence of any concomitant reactivity to glomerular substrate significantly boosted their pathogenic potential, as signified by the elevated proteinuria and azotemia triggered by these Abs.

Several investigators have already noted in the past that ANAs that also exhibited glomerular reactivity were significantly more pathogenic, both in murine models and in human systemic lupus erythematosus (4, 35–39). Using a multivariate analysis of parameters relating to 12 monoclonal ANAs, Gilkeson et al. have reported that in vitro glomerular reactivity was the parameter with the best predictive value for renal disease (37). They had also reported that

the glomerular binding exhibited by most anti-dsDNA ANAs was sensitive to DNase-I treatment. Thus, the present findings are consistent with the prevailing notion that the glomerular reactivity of most Abs may be dependent on the presence of nuclear antigenic bridges (40–42). On the other hand, polyreactive Abs and Abs that reacted directly with intrinsic glomerular antigens have also been shown to be nephritogenic (4, 43–48). Importantly, in addition to ANAs, polyreactive Abs, as well as Abs with specificity for the extracellular matrix are evidently more prominent in the glomerular deposits of lupus kidneys (47–49).

It is reasonable to posit that the Abs with nephrophilicity (irrespective of whether or not their glomerular binding is mediated by nuclear antigenic bridges) may be the most pathogenic because they may possess the greatest potential to "latch" onto the glomerular basement membrane or matrix. This could contribute to proteinuria in at least two ways. First, the massive coating of the filtration barrier with the nephrophilic Abs may compromise the charge barrier to glomerular filtration, thus allowing serum proteins to be lost. Second, the bound Abs may facilitate downstream Fc-dependent pathogenic cascades to proceed most effectively. Although both IgM and IgG Abs have the potential to fix complement, only the IgG Abs have the capacity to engage FcR-dependent events, such as those that serve to recruit macrophages and neutrophils from the systemic circulation. The critical role that these events play in engineering immune-mediated nephritis is clearly demonstrated by the phenotypes observed in FcR-deficient mice (50). This difference may explain why nephrophilic ANAs of the IgG isotype appear to be more pathogenic than those of the IgM isotype in the present work. However, one cannot exclude the possibility that differences in avidity for the glomerular substrate may also be contributing to the observed differences in pathogenicity between the two groups of Abs examined in this paper.

At the other end of the spectrum, the antinucleosome ANAs appear to be relatively harmless, owing perhaps to the fact that they do not bind avidly to anioinic antigenic substrates, such as DNA or the glomerular matrix. It is conceivable that this species of ANAs only acquires pathogenicity when coadministered with nucleosomes, which can serve as antigenic bridges for glomerular binding (19, 42). Finally, nonnephrophilic anti-dsDNA ANAs appear to have an intermediate phenotype in terms of their pathogenic potential. With respect to this observation, one could envisage two possibilities. First, one could hypothesize that although these Abs do not exhibit any nephrophilicity in vitro, they may possess varying degrees of nephrophilicity in vivo, perhaps mediated by nuclear antigenic bridges. Alternatively, they may use other means of in vivo pathogenicity as has been suggested (51, 52).

The findings reported in this paper have important ramifications in clinical diagnostics. Presently, several vendors market antinucleosome ELISA kits, promoting these Abs as being a better predictor of disease in systemic lupus erythematosus. Unfortunately, the antinucleosome ELISA detects both the anti-dsDNA Abs (that are pathogenic) as well as

the non-dsDNA binders (that are evidently not pathogenic). Therefore, the results of these tests should be considered in conjunction with the results of the anti-dsDNA ELISA. Thus, the presence of serum antinucleosome Abs in the absence of anti-dsDNA Abs may be an indicator of good prognosis. Indeed, genetic evidence for this notion has recently been advanced (11). On the other hand, testing for glomerular-binding specificities may be particularly useful in identifying patients with worse prognosis, which has been described previously (35, 36).

Another important contribution of this work revolves around the molecular structure of ANAs; in particular, the following observations are noteworthy. First, several of the observed features, including the IgM isotype, the increased *VH5/7183 VH* family usage (with the attendant differences in the amino acid usage at certain CDR positions), and their polyreactive specificity profiles are all reminiscent of the signatures of "natural autoantibodies" typically produced by B1 cells (53–55). The NZM2410 strain is known to harbor a massively enlarged B1 cell pool, both in the spleens as well as in the peritoneum, largely as a consequence of the lupus susceptibility locus, *Sle2* (56). Therefore, it is perhaps not surprising that approximately one fourth of the Abs rescued from NZM2410 mice possessed these signatures, presumably representing the products of B1 cells. Interestingly, approximately one third of the *VH5/7183*-encoded Abs were dsDNA/glomeruli dual reactive, whereas most of the rest were IgM antihistone/nucleosome Abs. It should be pointed out that most of these features, including the usage frequencies of *VH5/7183*, are very similar to the observations made with ANAs derived from the BWF1 lupus strain, another model that exhibits prominent B1 cell expansion (20).

With the aforementioned exception, the rescued ANAs and non-ANAs exhibited almost identical *VH* and *Vk* gene usages, similar *Jk* usage profiles, HC CDR3 and LC CDR1 lengths, mutation frequencies, as well as similar usage frequencies of almost all residues at most CDR positions. In earlier comparative papers (20–25, 57, 58), some of those features have been reported to apparently distinguish ANAs from non-ANAs; however, it remains possible that some of the latter differences may be the consequence of using the Kabat database as a normal control. Indeed, when we compared the CDR regions of NZM2410-derived ANA HCs with the Kabat database of normal HCs, a total of 39 residue differences were noted at a significance level of $P < 0.05$ (with 16 of these exceeding the threshold of $P < 0.001$), including several differences that involved nonpolar, conservative changes (unpublished data). The corresponding statistic for the LC comparisons (i.e., NZM2410-derived ANAs vs. Kabat database) was 49 ($P < 0.05$) and 13 ($P < 0.001$) residues, respectively.

In a recent analysis in which all murine ANAs rescued thus far were pooled and compared, although several "trends" were noted in the CDR2 regions of ANAs, most of these differences fell short of statistical significance; the only difference of prominence was noted at H52, where non-ANAs (from the Kabat database) had significantly

more D residues, compared with the ANAs (25). This reported difference coincides with the only significant HC CDR2 difference noted in the present work, where the NZM2410-derived ANAs exhibit more S residues than non-ANAs, apparently as a consequence of differences in *VH* germline gene usage. As site-directed mutagenesis studies have revealed that polar residues in the vicinity of H52 can potentially impact DNA binding (59), it is reasonable to posit that the residue differences noted at H52 may be the result of DNA-driven selection of *VH* germline genes that possess polar residues at these positions.

In contrast with the aforementioned residue differences, the sequence differences observed in ANA HC CDR3 regions were truly unmistakable. Previous investigators have observed that the HC of ANAs were more cationic due to the possession of R residues (20–25, 33, 57, 58, 60–62). Computer modeling papers have accorded potentially important roles for CDR3 R residues in making contact with nuclear antigens (63, 64). In addition, crystal structure analyses have elegantly portrayed the different mechanisms through which CDR3 R residues might facilitate DNA binding (65–69). Finally, a couple of groups have directly confirmed that targeted mutagenesis of R at H96 indeed mitigates DNA-binding (59, 70).

In studying a large panel of BWF1-derived ANAs, Marion and colleagues reported that the increased prominence of R residues at H98–H100a was a hallmark of ANAs (57–58). In addition, this work also revealed that the CDR3 regions of ANA HC had significantly fewer R residues at H97, suggesting that an R at H97 might actually destabilize key structural features of the antigen-binding groove, thus precluding dsDNA reactivity (58). In collecting and analyzing all murine ANAs characterized to date, Chen et al. reported that these patterns (i.e., increased R at H96 and H98–H100a, but not at H97) were key features of anti-ssDNA and anti-dsDNA Abs, but not antinucleosome Abs (25). In further support of these findings, crystal structure analysis of an anti-dsDNA Ab, Jel72, revealed that its CDR3 R residues at H98-H100a were indeed extending into the major groove of the cognate dsDNA target (69). Finally, the critical role played by R residues at H100 has been directly demonstrated by site-directed mutagenesis works (61, 71, 72). In contrast to the proposed role of charged residues at the aforementioned CDR3 positions, cationicity did not appear to be important at H95 (72). By analyzing ANAs and non-ANAs rescued from the same mice, the present paper confirms the aforementioned findings and further uncovers an intriguing CDR3 motif among the ANAs, in the aggregate, distinguished by alternating peaks of cationicity.

Aside from the contribution of the HC, it appears likely that the LC partner may also be playing a role in modulating DNA binding, as has been described previously (73–78). As an example, the nucleosome binder, ZDB4, fails to bind dsDNA, despite possessing R residues at H98 and H100 (Tables I and III). Interestingly, it possessed a rather anionic LC partner with D/E residues in CDR1 (L27 and L27c), CDR2 (L55), and CDR3 (L93 and L94). It is tempting to postulate that this LC partner might have ve-

toed dsDNA binding, as has been described for other LC partners (76). On the other hand, the strong dsDNA binder, ZDD1, exhibited no R/K residues in all three of its HC CDR regions and had a rather innocuous-looking CDR3 sequence, "GTGTGFAY"; interestingly, its LC partner possessed R residues in CDR2 (L54) and CDR3 (L96). It is tempting to posit that this LC partner might have been an important factor in conferring DNA reactivity to ZDD1. Finally, the potential contributions of LC in modulating reactivity to different nuclear antigens (i.e., dsDNA vs. nucleosomes) is also evident from the observed clonal relationships among the rescued ANAs (Fig. 8).

To conclude, although anti-dsDNA ANAs may be pathogenic, it is clear that nephrophilic isolates among these Abs (most of which bind glomerular substrate via nuclear antigenic bridges) are evidently the most pathogenic. In contrast, antinucleosome Abs appear to be rather innocuous. In addition, these studies suggest that ANAs and non-ANAs may be fairly similar in HC and LC structure and sequence, with a few major differences; cationic residues were particularly prominent at the alternating HC CDR3 positions, H96, H98, and H100, whereas these residues appeared to be excluded from the intervening positions, H97 and H99. The positioning of polar residues at specific CDR regions of ANAs may be the consequence of altered germline gene usage (as suggested by the observed differences at H52), or somatic mutations (as suggested by the differences noted at H31, H50, and H56). Clearly, the biological significance of these intriguing motifs and CDR residue differences needs to be verified using expression and mutagenesis studies.

References

1. Kotzin, B.L. 1996. Systemic lupus erythematosus. *Cell.* 85: 303–306.
2. Hahn, B.H. 1998. Antibodies to DNA. *N. Engl. J. Med.* 338: 1359–1368.
3. Pisetsky, D.H. 2000. Anti-DNA and autoantibodies. *Curr. Opin. Rheumatol.* 12:364–368.
4. Lefkowith, J.B., and G.S. Gilkeson. 1996. Nephritogenic autoantibodies in lupus. Current concepts and continuing controversies. *Arthritis Rheum.* 39:894–903.
5. Vlahakos, D.V., M.H. Foster, S. Adams, M. Katz, A.A. Ucci, K.J. Barrett, S.K. Datta, and M.P. Madaio. 1992. Anti-DNA antibodies form immune deposits at distinct glomerular and vascular sites. *Kidney Int.* 41:1690–1700.
6. Ohnishi, K., F.M. Ebling, B. Mitchell, R.R. Singh, B.H.

Hahn, and B.P. Tsao. 1994. Comparison of pathogenic and non-pathogenic murine antibodies to DNA: antigen binding and structural characteristics. *Int. Immunol.* 6:817–830.

7. Swanson, P.C., R.L. Yung, N.B. Blatt, M.A. Eagan, J.M. Norris, B.C. Richardson, K.J. Johnson, and G.D. Glick. 1996. Ligand recognition by murine anti–DNA autoantibodies. II. Genetic analysis and pathogenicity. *J. Clin. Invest.* 97:1748–1760.

8. Spatz, L., A. Iliev, V. Saenko, L. Jones, M. Irigoyen, A. Manheimer-Lory, B. Gaynor, C. Putterman, M. Bynoe, C. Kowal, et al. 1997. Studies on the structure, regulation, and pathogenic potential of anti-dsDNA antibodies. *Methods.* 11: 70–78.

9. Rubin, R.L., S.A. Bell, and R.W. Burlingame. 1992. Autoantibodies associated with lupus induced by diverse drugs target a similar epitope in the (H2A-H2B)-DNA complex. *J. Clin. Invest.* 90:165–173.

10. Monestier, M., and B.L. Kotzin. 1992. Antibodies to histones in systemic lupus erythematosus and drug-induced lupus syndromes. *Rheum. Dis. Clin. North Am.* 18:415–436.

11. Mohan, C., F. Liu, C. Xie, and R. Williams. 2001. Antisubnucleosome reactivities in SLE patients and their first degree relatives. *Clin. Exp. Immunol.* 123:119–126.

12. Burlingame, R.W., R.L. Rubin, R.S. Balderas, and A.N. Theofilopoulos. 1993. Genesis and evolution of antichromatin autoantibodies in murine lupus implicates T-dependent immunization with self antigen. *J. Clin. Invest.* 91:1687–1696.

13. Burlingame, R.W., M.L. Boey, G. Starkebaum, and R.L. Rubin. 1994. The central role of chromatin in autoimmune responses to histones and DNA in systemic lupus erythematosus. *J. Clin. Invest.* 94:184–192.

14. Amoura, Z., H. Chabre, S. Koutouzov, C. Lotton, A. Cabrespines, J.F. Bach, and L. Jacob. 1994. Nucleosome-restricted antibodies are detected before anti–dsDNA and/or antihistone antibodies in serum of MRL-Mp lpr/lpr and +/+ mice, and are present in kidney eluates of lupus mice with proteinuria. *Arthritis Rheum.* 37:1684–1688.

15. Mohan, C., E. Alas, L. Morel, P. Yang, and E.K. Wakeland. 1998. Genetic dissection of SLE pathogenesis. Sle1 on murine chromosome 1 leads to a selective loss of tolerance to H2A/H2B/DNA subnucleosomes. *J. Clin. Invest.* 101:1362–1372.

16. Mohan, C., L. Morel, P. Yang, H. Watanabe, B. Croker, G. Gilkeson, and E.K. Wakeland. 1999. Genetic dissection of lupus pathogenesis: a recipe for nephrophilic autoantibodies. *J. Clin. Invest.* 103:1685–1695.

17. Shi, X., C. Xie, J. Richardson, and C. Mohan. 2002. Genetic dissection of SLE: *Sle1* and *Fas* impact distinct pathways leading to lymphoproliferative autoimmunity. *J. Exp. Med.* 196: 281–292.

18. Morel, L., B.P. Croker, K.R. Blenman, C. Mohan, G. Huang, G. Gilkeson, and E.K. Wakeland. 2000. Genetic reconstitution of systemic lupus erythematosus immunopathology with polycongenic murine strains. *Proc. Natl. Acad. Sci. USA.* 97:6670–6675.

19. van Bruggen, M.C., B. Walgreen, T.P. Rijke, W. Tamboer, K. Kramers, R.J. Smeenk, M. Monestier, G.J. Fournie, and J.H. Berden. 1997. Antigen specificity of anti-nuclear antibodies complexed to nucleosomes determines glomerular basement membrane binding in vivo. *Eur. J. Immunol.* 27: 1564–1569.

20. Marion, T.N., D.M. Tillman, N.T. Jou, and R.J. Hill. 1992. Selection of immunoglobulin variable regions in autoimmunity to DNA. *Immunol. Rev.* 128:123–149.

21. Radic, M.Z., and M. Weigert. 1994. Genetic and structural evidence for antigen selection of anti-DNA antibodies. *Annu. Rev. Immunol.* 12:487–520.

22. Eilat, D., and W.F. Anderson. 1994. Structure-function correlates of autoantibodies to nucleic acids. Lessons from immunochemical, genetic and structural studies. *Mol. Immunol.* 31:1377–1390.

23. Lefkowith, J.B., R.D. Valerio, J. Norris, G.D. Glick, A.L. Alexander, L. Jackson, and G.S. Gilkeson. 1996. Murine glomerulotrophic monoclonal antibodies are highly oligoclonal and exhibit distinctive molecular features. *J. Immunol.* 157:1297–1305.

24. Koutouzov, S., F. Jovelin, F. Brard, G. Raux, F. Tron, and D. Gilbert. 1997. Comparison of structural characteristics of antisubnucleosome and anti-DNA monoclonal antibodies derived from lupus mice. *Ann. NY Acad. Sci.* 815:327–330.

25. Chen, L., S. Chang, and C. Mohan. 2002. Molecular signatures of anti-ssDNA, anti-dsDNA, and anti-nucleosome autoantibody heavy chains. *Mol. Immunol.* 39:333–347.

26. Liang, Z., C. Chen, and C. Mohan. 2003. Molecular signatures of anti-nuclear antibodies: contributions of specific light chain residues and a novel NZB $V_k 1$ germline gene. *J. Immunol.* 171:3886–3894.

27. Rudofsky, U.H., B.D. Evans, S.L. Balaban, V.D. Mottironi, and A.E. Gabrielsen. 1993. Differences in expression of lupus nephritis in New Zealand mixed H-2z homozygous inbred strains of mice derived from New Zealand black and New Zealand white mice. Origins and initial characterization. *Lab. Invest.* 68:419–426.

28. Morel, L., X.H. Tian, B.P. Croker, and E.K. Wakeland. 1999. Epistatic modifiers of autoimmunity in a murine model of lupus nephritis. *Immunity.* 11:131–139.

29. Bynoe, M.S., L. Spatz, and B. Diamond. 1999. Characterization of anti-DNA B cells that escape negative selection. *Eur. J. Immunol.* 29:1304–1313.

30. Xie, C., J.X. Zhou, and C. Mohan. 2003. Enhanced intrinsic susceptibility to nephritis in the lupus facilitating NZW strain. *Arthritis Rheum.* 48:1080–1092.

31. Zhou, X.J., Z. Laszik, X.Q. Wang, F.G. Silva, and N.D. Vaziri. 2000. Association of renal injury with increased oxygen free radical activity and altered nitric oxide metabolism in chronic experimental hemosiderosis. *Lab. Invest.* 80:1905–1914.

32. Benson, J.R. 1977. Improved ion-exchange resins. *Methods Enzymol.* 47:19–31.

33. Shlomchik, M., M. Mascelli, H. Shan, M.Z. Radic, D. Pisetsky, A. Marshak Rothstein, and M. Weigert. 1990. Anti-DNA antibodies from autoimmune mice arise by clonal expansion and somatic mutation. *J. Exp. Med.* 171:265–292.

34. Diamond, B., J.B. Katz, E. Paul, C. Aranow, D. Lustgarten, and M.D. Scharff. 1992. The role of somatic mutation in the pathogenic anti-DNA response. *Annu. Rev. Immunol.* 10: 731–757.

35. Budhai, L., K. Oh, and A. Davidson. 1996. An in vitro assay for detection of glomerular binding IgG autoantibodies in patients with systemic lupus erythematosus. *J. Clin. Invest.* 98: 1585–1593.

36. Lefkowith, J.B., M. Kiehl, J. Rubenstein, R. DiValerio, K. Bernstein, L. Kahl, R.L. Rubin, and M. Gourley. 1996. Heterogeneity and clinical significance of glomerular-binding antibodies in systemic lupus erythematosus. *J. Clin. Invest.* 98:

1373–1380.

37. Gilkeson, G.S., K. Bernstein, A.M. Pippen, S.H. Clarke, T. Marion, D.S. Pisetsky, P. Ruiz, and J.B. Lefkowith. 1995. The influence of variable-region somatic mutations on the specificity and pathogenicity of murine monoclonal anti-DNA antibodies. *Clin. Immunol. Immunopathol.* 76:59–67.

38. Vargas, M.T., K. Gustilo, D.M. D'Andrea, R. Kalluri, M.H. Foster, and M.P. Madaio. 1997. Structural features of nephritogenic lupus autoantibodies. *Methods.* 11:62–69.

39. Raz, E., M. Brezis, E. Rosenmann, and D. Eilat. 1989. Anti-DNA antibodies bind directly to renal antigens and induce kidney dysfunction in the isolated perfused rat kidney. *J. Immunol.* 40:3076–3082.

40. Di Valerio, R., K.A. Bernstein, E. Varghese, and J.B. Lefkowith. 1995. Murine lupus glomerulotropic monoclonal antibodies exhibit differing specificities but bind via a common mechanism. *J. Immunol.* 155:2258–2268.

41. Bernstein, K.A., R.D. Valerio, and J.B. Lefkowith. 1995. Glomerular binding activity in MRL lpr serum consists of antibodies that bind to a DNA/histone/type IV collagen complex. *J. Immunol.* 154:2424–2433.

42. Kramers, C., M.N. Hylkema, M.C. van Bruggen, R. van de Lagemaat, H.B. Dijkman, K.J. Assmann, R.J. Smeenk, and J.H. Berden. 1994. Anti-nucleosome antibodies complexed to nucleosomal antigens show anti-DNA reactivity and bind to rat glomerular basement membrane in vivo. *J. Clin. Invest.* 94:568–577.

43. Foster, M.H., B. Cizman, and M.P. Madaio. 1993. Nephritogenic autoantibodies in systemic lupus erythematosus: immunochemical properties, mechanisms of immune deposition, and genetic origins. *Lab. Invest.* 69:494–507.

44. Foster, M.H., J. Sabbaga, S.R. Line, K.S. Thompson, K.J. Barrett, and M.P. Madaio. 1993. Molecular analysis of spontaneous nephrotropic anti-laminin antibodies in an autoimmune MRL-lpr/lpr mouse. *J. Immunol.* 151:814–824.

45. Wick, G., P.U. Muller, and R. Timpl. 1982. In vivo localization and pathological effects of passively transferred antibodies to type IV collagen and laminin in mice. *Clin. Immunol. Immunopathol.* 23:656–665.

46. Deocharan, B., X. Qing, J. Lichauco, and C. Putterman. 2002. Alpha-actinin is a cross-reactive renal target for pathogenic anti-DNA antibodies. *J. Immunol.* 168:3072–3078.

47. Pankewycz, O.G., P. Migliorini, and M.P. Madaio. 1987. Polyreactive autoantibodies are nephritogenic in murine lupus nephritis. *J. Immunol.* 139:3287–3294.

48. Van Bruggen, M.C., C. Kramers, M.N. Hylkema, R.J. Smeenk, and J.H. Berden. 1996. Significance of anti-nuclear and anti-extracellular matrix autoantibodies for albuminuria in murine lupus nephritis; a longitudinal study on plasma and glomerular eluates in MRL/l mice. *Clin. Exp. Immunol.* 105:132–139.

49. Xie, C., E. Liang, and C. Mohan. 2003. Use of a novel elution regime reveals the dominance of cross-reactive anti-dsDNA autoantibodies in lupus kidneys. *Arthritis Rheum.* 48:2343–2352.

50. Clynes, R., C. Dumitru, and J.V. Ravetch. 1998. Uncoupling of immune complex formation and kidney damage in autoimmune glomerulonephritis. *Science.* 279:1052–1054.

51. Vlahakos, D., M.H. Foster, A.A. Ucci, K.J. Barrett, S.K. Datta, and M.P. Madaio. 1992. Murine monoclonal anti-DNA antibodies penetrate cells, bind to nuclei, and induce glomerular proliferation and proteinuria in vivo. *J. Am. Soc. Nephrol.* 2:1345–1354.

52. Ternynck, T., A. Avrameas, J. Ragimbeau, G. Buttin, and S. Avrameas. 1998. Immunochemical, structural and translocating properties of anti-DNA antibodies from (NZBxNZW)F1 mice. *J. Autoimmun.* 11:511–521.

53. Diaw, L., C. Magnac, O. Pritsch, M. Buckle, P. Alzari, and G. Dighiero. 1997. Structural and affinity studies of IgM polyreactive natural autoantibodies. *J. Immunol.* 158:968–976.

54. Holmberg, D. 1987. High connectivity, natural antibodies preferentially use 7183 and QUPC 52 VH families. *Eur. J. Immunol.* 17:399–407.

55. Pennell, C.A., L.W. Arnold, G. Haughton, and S.H. Clarke. 1988. Restricted Ig variable region gene expression among Ly-1+ B cell lymphomas. *J. Immunol.* 141:2788–2796.

56. Mohan, C., L. Morel, P. Yang, and E.K. Wakeland. 1998. Accumulation of splenic B1a cells with potent antigen-presenting capability in NZM2410 lupus-prone mice. *Arthritis Rheum.* 41:1652–1662.

57. Tillman, D.M., N.T. Jou, R.J. Hill, and T.N. Marion. 1992. Both IgM and IgG anti-DNA antibodies are the products of clonally selective B cell stimulation in (NZB × NZW)F1 mice. *J. Exp. Med.* 176:761–779.

58. Krishnan, M.R., N.T. Jou, and T.N. Marion. 1996. Correlation between the amino acid position of arginine in VH-CDR3 and specificity for native DNA among autoimmune antibodies. *J. Immunol.* 157:2430–2439.

59. Radic, M.Z., J. Mackle, J. Erikson, C. Mol, W.F. Anderson, and M. Weigert. 1993. Residues that mediate DNA binding of autoimmune antibodies. *J. Immunol.* 150:4966–4977.

60. Gilkeson, G.S., D.D. Bloom, D.S. Pisetsky, and S.H. Clarke. 1993. Molecular characterization of anti-DNA antibodies induced in normal mice by immunization with bacterial DNA. Differences from spontaneous anti-DNA in the content and location of VH CDR3 arginines. *J. Immunol.* 151:1353–1364.

61. Wloch, M.K., S.H. Clarke, and G.S. Gilkeson. 1997. Influence of VH CDR3 arginine and light chain pairing on DNA reactivity of a bacterial DNA-induced anti-DNA antibody from a BALB/c mouse. *J. Immunol.* 159:6083–6090.

62. Kieber, E.T., M.H. Foster, W.V. Williams, and M.P. Madaio. 1994. Structural properties of a subset of nephritogenic anti-DNA antibodies. *Immunol. Res.* 13:172–185.

63. Seeman, N.C., J.M. Rosenberg, and A. Rich. 1976. Sequence-specific recognition of double helical nucleic acids by proteins. *Proc. Natl. Acad. Sci. USA.* 73:804–808.

64. McClarin, J.A., C.A. Frederick, B.C. Wang, P. Greene, H.W. Boyer, J. Grable, and J.M. Rosenberg. 1986. Structure of the DNA-Eco RI endonuclease recognition complex at 3 A resolution. *Science.* 234:1526–1541.

65. Herron, J.N., X.M. He, D.W. Ballard, P.R. Blier, P.E. Pace, A.L. Bothwell, E.W.J. Voss, and A.B. Edmundson. 1991. An autoantibody to single-stranded DNA: comparison of the three-dimensional structures of the unliganded Fab and a deoxynucleotide-Fab complex. *Proteins.* 11:159–175.

66. Cygler, M., A. Boodhoo, J.S. Lee, and W.F. Anderson. 1987. Crystallization and structure determination of an autoimmune anti-poly(dT) immunoglobulin Fab fragment at 3.0 A resolution. *J. Biol. Chem.* 262:643–648.

67. Pokkuluri, P.R., F. Bouthillier, Y. Li, A. Kuderova, J. Lee, and M. Cygler. 1994. Preparation, characterization and crystallization of an antibody Fab fragment that recognizes RNA. Crystal structures of native Fab and three Fab-mononucleotide complexes. *J. Mol. Biol.* 243:283–297.

68. Barry, M.M., C.D. Mol, W.F. Anderson, and J.S. Lee. 1994. Sequencing and modeling of anti-DNA immunoglobulin Fv

domains. Comparison with crystal structures. *J. Biol. Chem.* 269:3623–3632.

69. Tanner, J.T., A.A. Komissarov, and S.L. Deutscher. 2001. Crystal structure of an antigen-binding fragment bound to single-stranded DNA. *J. Mol. Biol.* 314:807–822.

70. Katz, J.B., W. Limpanasithikul, and B. Diamond. 1994. Mutational analysis of an autoantibody: differential binding and pathogenicity. *J. Exp. Med.* 180:925–932.

71. Martin, T., R. Crouzier, J.C. Weber, T.J. Kipps, and J.L. Pasquali. 1994. Structure-function studies on a polyreactive (natural) autoantibody. Polyreactivity is dependent on somatically generated sequences in the third complementarity-determining region of the antibody heavy chain. *J. Immunol.* 152:5988–5996.

72. Radic, M.Z., and S.N. Seal. 1997. Selection of recurrent V genes and somatic mutations in autoantibodies to DNA. *Methods.* 11:20–26.

73. Diamond, B., and D. Eilat. 1997. DNA antibodies focus on the light chain. *Lupus.* 6:315–316.

74. Radic, M.Z., M.A. Mascelli, J. Erikson, H. Shan, and M. Weigert. 1991. Ig H and L chain contributions to autoimmune specificities. *J. Immunol.* 146:176–182.

75. Ibrahim, S.M., M. Weigert, C. Basu, J. Erikson, and M.Z. Radic. 1995. Light chain contribution to specificity in anti-DNA antibodies. *J. Immunol.* 155:3223–3233.

76. Li, H., Y. Jiang, E.L. Prak, M.Z. Radic, and M. Weigert. 2002. Editors and editing of anti-DNA receptors. *Immunity.* 15:947–957.

77. Fitzsimons, M.M., H. Chen, and M.H. Foster. 2000. Diverse endogenous light chains contribute to basement membrane reactivity in nonautoimmune mice transgenic for an anti-laminin Ig heavy chain. *Immunogenetics.* 51:20–29.

78. Spatz, L., V. Saenko, A. Iliev, L. Jones, L. Geskin, and B. Diamond. 1997. Light chain usage in anti-double-stranded DNA B cell subsets: role in cell fate determination. *J. Exp. Med.* 185:1317–1326.